THE UNIVERSITY OF MICHIGAN

COLLEGE OF ENGINEERING
Department of Electrical Engineering
Plasma Engineering Laboratory

Final Report

PLASMA MEASUREMENTS FROM 3 TO 120 KILOBARS OF PRESSURE

James W. Robinson

Approved by: H. C. Early

ORA Project 05742

supported by:

NATIONAL AERONAUTICS AND SPACE ADMINISTRATION
GRANT NO. NsG-415
WASHINGTON, D. C.

administered through:

OFFICE OF RESEARCH ADMINISTRATION ANN ARBOR

May 1966

TABLE OF CONTENTS

	Page
SUMMARY	1
INTRODUCTION	1
I. EXPERIMENTAL PROCEDURE	3
Equipment	3
Auxiliary Tests	5
Initiating the Discharge	6
II. PRESSURE	9
Mechanical Restraint of Expanding Column	9
Pinch Pressure	13
III. EXPERIMENTS WITHOUT EXPLOSIVE	15
Special Electrode Design	15
Effect of Dissolved Air	15
Calculations	17
Results	17
IV. EXPERIMENTS WITH EXPLOSIVE	24
Calculations	24
Results	24
Irregularities	28
CONCLUSIONS	31
APPENDIX	32
REFERENCES	43

PLASMA MEASUREMENTS FROM 3 TO 120 KILOBARS OF PRESSURE

By James W. Robinson
The University of Michigan

SUMMARY

Measurements of pressure, temperature, resistivity, and energy density have been made for plasmas at pressures ranging from 3 to 120 kilobars and at temperatures of 10 000°K and 35 000°K. These plasmas have particle densities up to 10^{23} cm^{-3}.

The plasmas were formed by discharging a capacitor bank between electrodes submerged in water. Pressures up to 15 kilobars were obtained in this way, where the main source of pressure was the magnetic pinch effect. The inertial restraint of the plasma by water surrounding the discharge path also contributed to the pressure. For pressures up to 120 kilobars, a chemical explosive was detonated in the water near the electrical discharge path. The shock wave from the explosive established a region of water compressed to 100 kilobars, in which the column of plasma was formed.

The data for resistivity and energy density show resistivity decreasing with increasing pressure, and energy density increasing. At the lower pressures, the energy density is about 5 times that predicted by calculations based upon the Debye shielding theory. Because of the close spacing of the ions, their interactions can properly be analyzed only with quantum mechanics.

INTRODUCTION

During the final phases of this research program on plasmas at high pressure, large amounts of experimental data have been obtained. Plasmas have been investigated at pressures ranging from 3 to 120 kilobars and at temperatures of 10 000°K and 35 000°K. Variations of resistivity and energy density with pressure have need determined from computations based upon the data. A previous report on this work described the experimental procedures in detail, presented data for a few experimental conditions, and discussed the theory of the plasmas (1). In the present report, the emphasis is upon experimental results; procedures are discussed briefly, for completeness, and some improvements in the experimental methods are described.

Plasmas in the lower portion of the pressure range are formed by discharging a bank of energy-storage capacitors between electrodes submerged in water.

The pressure results from the combined effects of the magnetic pinch forces and of the inertial restraint of the plasma by the water surrounding the discharge column. For higher pressures, the same method is used, augmented by the detonation of a charge of chemical explosive in the water near the electrical discharge path. The shock wave from the explosive establishes a region of water compressed to 100 kilobars of pressure, in which the column of plasma is formed. As an alternative, the shock front may be made to sweep through an already formed column.

From the data recorded over an observation period of about 1 μsec, the temperature, pressure, resistivity, energy density, and dimensions of the discharge column are computed. From these results, trends can be identified and theoretical models of the plasma can be checked for their appropriateness.

Introductory work in using a discharge in a liquid as a tool for studying plasmas at high pressure was done by E. A. Martin (2). However, his measurements lacked resolution, and he neglected the important effects of cylindrical symmetry in the discharge column when computing pressure. The introduction of explosive charges and improvements in his methods have made possible the acquisition of data accurate enough to be compared with theoretical studies over a wide range of pressures.

Tests without chemical explosive were performed for each of several rates of current rise through the discharge column, ranging from 25 to 250 kA/μsec. At the lower rates, the pressure was produced primarily by the inertial effects of the water surrounding the discharge, whereas at the higher rates, the pressure was produced primarily by the magnetic pinch. Pressures ranged from 3 to 15 kilobars, and temperatures had nearly the same value, 35 000°K, in all cases.

A similar series of tests were performed with chemical explosive although the current range was not as great because of the higher resistance encountered in the discharge columns at the higher pressures. With temperatures of approximately 10 000°K, the discharge columns had pressures ranging from 100 to 120 kilobars, depending upon the pinch effect.

A fine wire is usually stretched between the electrodes to initiate the discharge. A method was found of eliminating the wire, although the method was not adopted for the experimental program.

Results of a computer calculation are included to show how plasma pressure is related to inertial restraint of the plasma by the surrounding water.

I. EXPERIMENTAL PROCEDURE

Equipment

The energy-storage capacitors for generating the plasma had to be located in the vicinity of detonating explosives. To avoid damage to the capacitors and other instrumentation, the nonexpendable items were separated by a plywood barricade from the test chamber, which was an open steel tank with 1 in. walls. The capacitor bank, which had 56.1 μF rated at 20 kV, was connected to the discharge electrodes in the tank by expendable copper straps, which were spaced closely to minimize inductance.

The electrode system used for much of the work is shown in Fig. 1. The entire system is immersed in water in the test chamber so that water flows into the spaces between and around the electrodes. The shock wave generated by the explosive is directed vertically, to compress the water in the vicinity of the initiating wire where the plasma is formed.

During each experiment, two photographs were taken with a specially designed camera having two Kerr cell shutters. A beam-splitting mirror behind the lens formed two images which could be shuttered independently by the two Kerr cells. Continuously variable delay circuits controlled the timing of the exposures. The shutters were operated by pulse-forming networks designed to open them for 0.1 μsec.

Data from the experiments were recorded by oscilloscopes. Discharge current was measured with a magnetic-flux sampling loop used with an integrating circuit which fed one oscilloscope channel. With one end of the discharge column at ground potential, the voltage of the high end was recorded on a second channel with a 1000X probe. Also the timing of the Kerr cell shutters was monitored on a third channel.

The discharge of the capacitor bank and the operation of the instruments were controlled by specially divised timing circuits. A sensor wire was buried in the explosive, as shown in Fig. 1. A pulse-generating circuit was actuated by the passage of the detonation front in the explosive over the sensor wire, and pulses were sent through appropriate delay circuits to initiate the other events in the experiment. One pulse was amplified to trigger a three-electrode spark gap which initiated the capacitor discharge. Another pulse operated the camera, and a third triggered the oscilloscopes. In tests without explosive, the pulse generator was triggered manually.

The data record from each experiment contained oscilloscope traces swept at 0.2 μsec/cm, a negative showing two Kerr cell photographs side by side, and

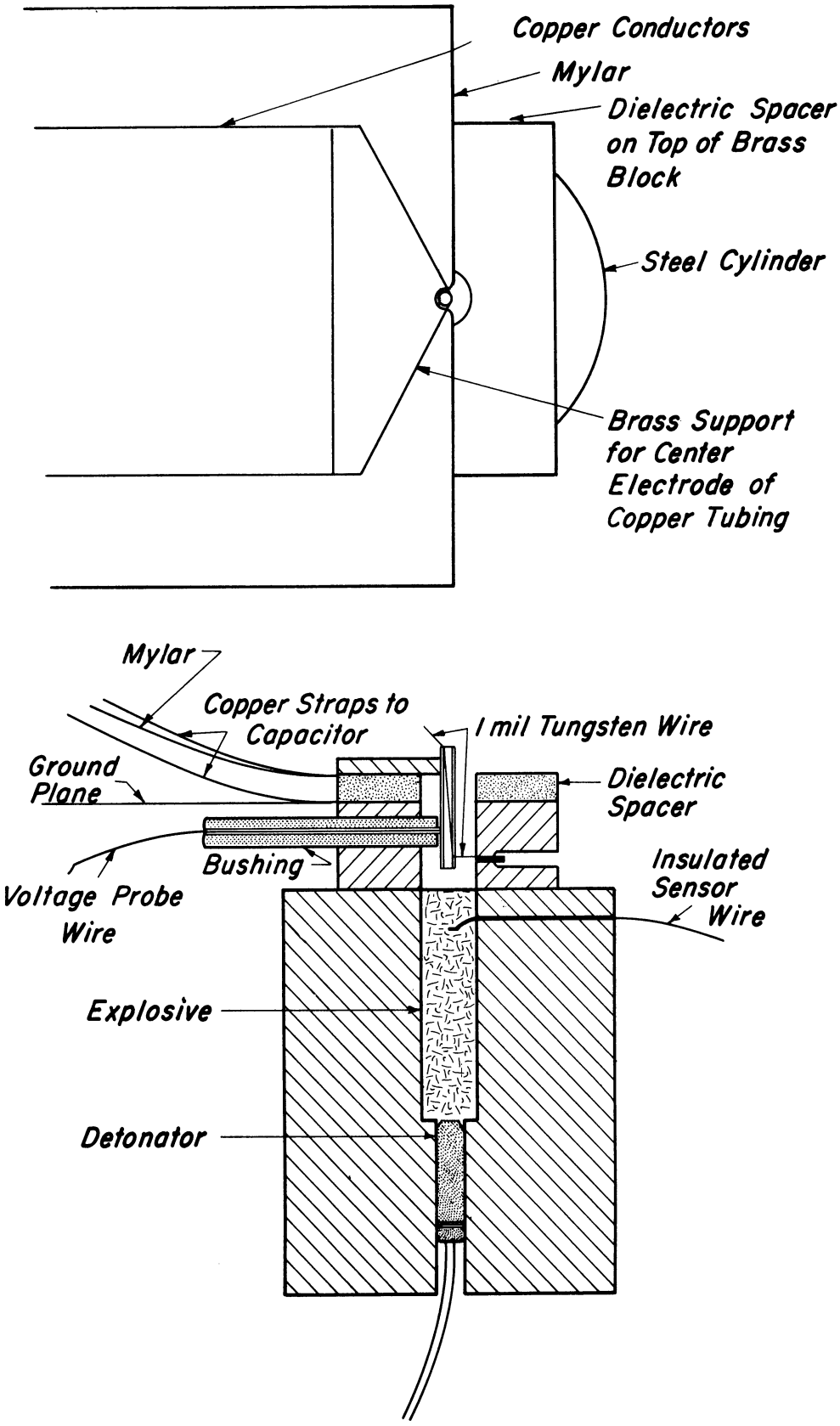

Fig. 1. Electrode assembly and explosive charge.

dimensions of the electrode system. The critical dimensions were the length of the discharge column, the distance of the discharge from the surface of the explosive, and the location of the sensor wire in the explosive.

Auxiliary Tests

Certain auxiliary tests were necessary for the correct interpretation of the experimental data. Among these was the calibration of the current-measuring system, for which the capacitor bank was discharged into a short circuit. From the resulting oscilloscope trace, the ring frequency and damping factor could be calculated. By combining this information with knowledge of capacitance and charging voltage, the peak discharge current could be computed, and from that the scaling factor for converting the signal voltage into discharge current.

Other tests were performed to relate the image density of the Kerr cell photographs to plasma temperature. The plasma radiates a blackbody spectrum. For a spectral band representing the response of the camera and film together, the relative intensity of radiation striking the film was computed as a function of temperature and f number of the lens. From photographs of a reference source at known temperature, the relationship among image density, f number, and temperature was then established.

An electrical discharge in water was selected as a reference. The temperature of the reference was determined by a procedure described in earlier reports, (1,2) in which absolute radiation intensity for a narrow spectral band is measured with a vacuum photodiode that has been calibrated against a tungsten ribbon at a known temperature. A density scale is exposed on the border of each sheet of film to serve, after calibration, as a scale of temperature. Although the use of film image density to indicate temperature is not highly accurate, the method does have the advantages of providing a temperature measurement with every experiment and of making it possible to identify temperature variations in a discharge column.

To measure the inductance of the discharge column and the electrodes, a heavy copper wire was substituted for the discharge column and voltage measurements were taken just as in tests with plasma formation. The voltage was 90° out of phase with current, as would be expected for an inductive load. Inductance was calculated, and corrected to allow for the difference between the inductance of the copper wire and that of the plasma column. On the basis of the results, the voltage measurements from tests with plasma formation were corrected by $d/dt(LI)$. In general, this correction was from 10 to 20% of the measured voltage.

The chemical explosive produces high pressure in a region of water between the explosive-water interface and the shock front that propagates from that

interface through the water. A unique relation exists between the velocity of the shock front and the pressure in the region behind the front (3). The pressure can therefore be computed from another auxiliary test, the measurement of shock velocity.

A series of tests with shock front sensors located at different distances from the surface of the explosive provides the data needed for computing pressure. The earlier report described a set of measurements in which transparent hollow wafers filled with argon were used as sensors (1, p. 16). When the shock struck the argon, a light flash was produced which was observed with a phototube and recorded with an oscilloscope. However, more precise measurements have been obtained with a different technique, and the use of an oscilloscope sweep speed correction factor has further improved the data.

The new technique uses a mechanical switch which consists of a metal foil that is driven against a pin by the shock front. The switching action itself is very abrupt although in some tests it was significantly delayed. From the newer data, the pressure is estimated to be 100 kilobars instead of 115 as previously reported.

Initiating the Discharge

The formation of the plasma column must be closely synchronized with the arrival of the explosively generated shock wave if the high and uniform pressure produced by the explosive is to be effectively utilized. Therefore the jitter in the formative time of the discharge path must be kept small. For electrodes 1/4 in. apart, the formative time at 20 kV was found to be from 1 to 2 μsec, with a jitter on the order of 1 μsec. When the discharge path formed, it was not straight, as desired, but it followed a random path. Hence it was necessary to establish a preferred breakdown path to obtain a uniformly shaped discharge as well as to control jitter.

The method generally used in this research was to stretch a fine wire between the electrodes. The breakdown path was then very straight and the formative jitter could be kept small. A very fine wire must be used in order to minimize the contamination of the plasma with metal ions. The ratio of metal to water in the plasma may be very small, but because of the low ion mobility the metal remains concentrated on the axis of the discharge column. For the same reason, electrode metal does not migrate a significant distance into the plasma. Wire of 0.001 in. tungsten was strong enough to be used without breaking frequently, and it showed negligible jitter. Wire of 0.0005 in. tungsten showed jitter of a few tenths of a microsecond, which was unacceptable. Copper was found to be superior to tungsten for controlling jitter, in that 0.0004 in. copper was satisfactory, but wire breakage caused some trouble.

Other methods of establishing a preferred discharge path were investigated, with limited success. The contamination from the wire was suspected of introducing irregularities into the plasmas, and ways were sought to eliminate them. Though irregularities still existed, a method was found which could be made to work with somewhat more effort than the use of a wire requires.

A vortex was formed in the water between the electrodes with a void along its axis. With an applied voltage of 40 kV, a fairly reproducible formative time of about 0.2 μsec was obtained. A system using the vortex with explosive is shown in Fig. 2. The cylindrical vortex chamber was made of transparent material so the plasma could be photographed, although a correction was necessary because of the optical distortion of the curved surface. The shock wave from the explosive propagated through the chamber wall into the swirling water, which was stationary on the time scale of the experiment. Water was injected tangentially through a pressure regulating valve, and exhausted through a No. 65 hole (0.035 in. dia) into a vacuum line.

Still other methods were considered. In one of them, a jet of hot, salty water was passed from a hole in one electrode over to the other, where it was sucked out through a second hole; thus a column of the more conductive water was surrounded by cool unsalted water. However, reliable breakdown could not be attained by this method. Sharply pointed electrodes were tried also.

One other method might work if equipment were available. If a pulsed laser beam were focused with a cylindrical lens to form a line image, the water at the image would be ionized and a preferred path for the discharge would be established.

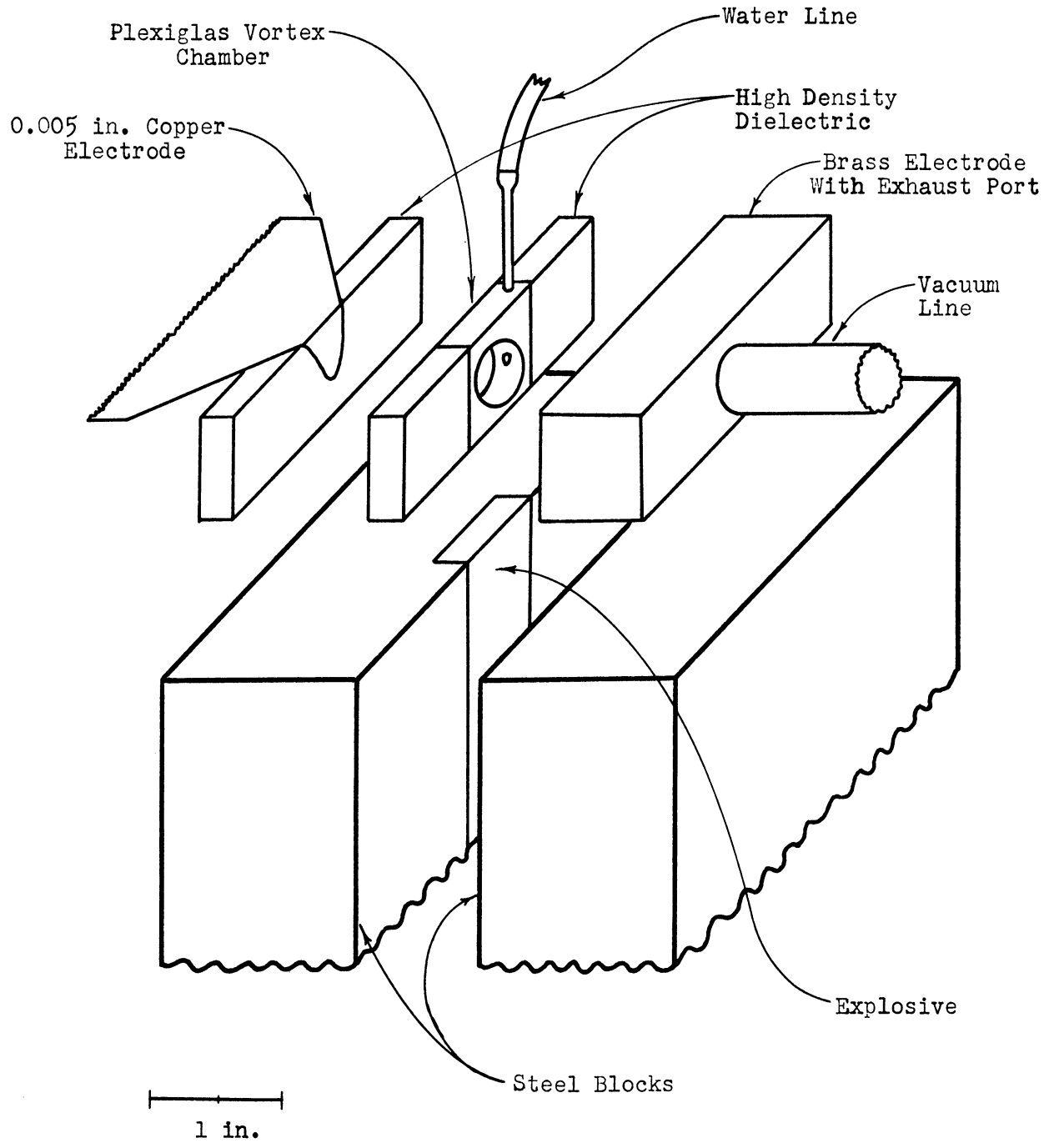

Fig. 2. Exploded view of electrode assembly using vortex to initiate discharge.

II. PRESSURE

Pressure develops because the expanding plasma column is mechanically restrained by the water surrounding it. Magnetic pinch forces also contribute. This section considers these two causes of pressure in turn.

Mechanical Restraint of Expanding Column

Ideally, the pressure is computed at the surface of a radially expanding cylinder in water, which initially has some uniform ambient pressure—either atmospheric pressure, without explosive; or 100 kilobars, with explosive. It is assumed that the pressure is uniform throughout the cylinder of plasma and that the rate of induction of water into the plasma at its boundary is negligible. Also, for the cases of interest in this work the radial growth rate is nearly constant, so that the simplifying assumption of constant growth rate can be made.

The earlier report described a calculation of the pressure produced by mechanical restraint (1, pp. 37-45). The above assumptions were used with some simplified equations which had obvious shortcomings but did give a first approximation of the effects of cylindrical symmetry. A more rigorous and extensive calculation has been made with a digital computer, and the results are presented here. The method is that of G. I. Taylor, which is described by Courant and Friedrichs (4, pp. 424-25).

The model for the calculation is a radially expanding cylinder which displaces water and generates a shock wave concentric with the cylinder, as shown in Fig. 3. The shock velocity, the mass velocity in the region of water between the cylinder and the shock front, and the density in the same region must be computed to determine the pressure at the surface of the cylinder. The basic equations are the equation of mass conservation, the equation of momentum conservation, and the equation of state of water.

The equation of state (4, p. 8) relating pressure p and density ρ is

$$p + B = (p_{oo}+B)(\rho/\rho_{oo})^{\gamma} = A\,\rho^{\gamma} \qquad (2.1)$$

where γ is 7, the subscript $_{oo}$ refers to water at 20°C and 1 atmosphere, and B is taken at 3140×10^5 N/m^2 to make the speed of sound in water consistent with its nominal value of 1483 m/sec. The speed of sound c is $(dp/d\rho)^{1/2}$.

With u representing mass velocity, the equations of mass and momentum conservation in cylindrical coordinates (4, p. 29) are

$$r(\partial\rho/\partial t) + \partial(ru\rho)/\partial r = 0 \qquad (2.2)$$

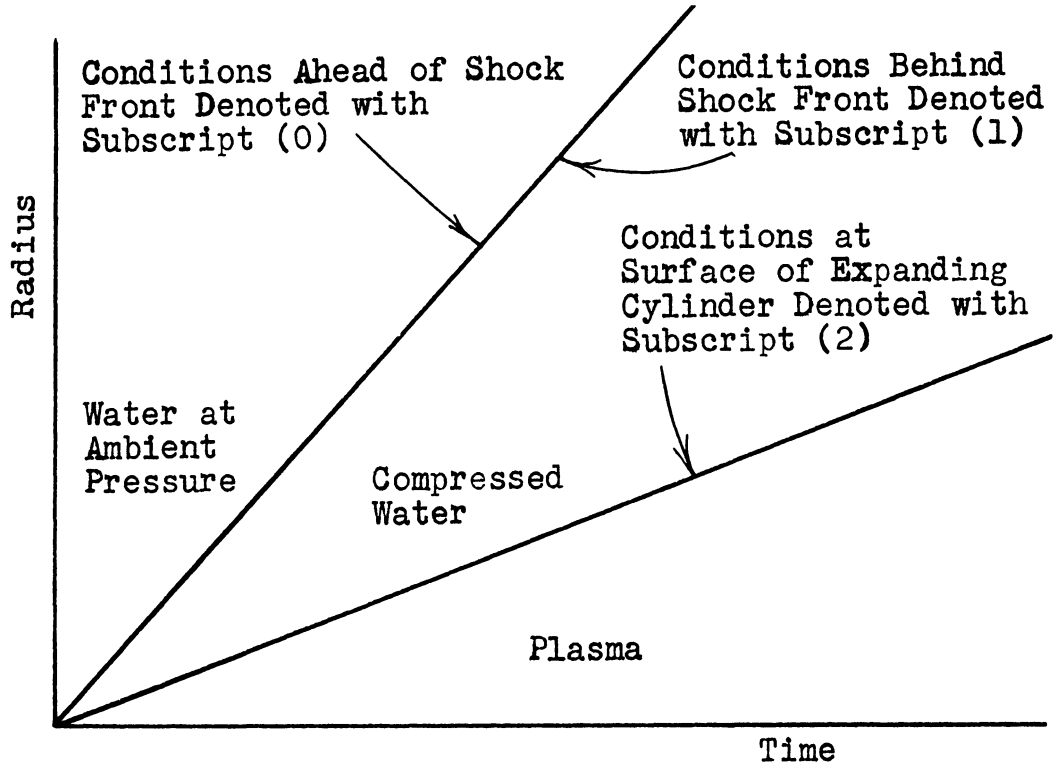

Fig. 3. Model of shock wave produced by expanding cylinder of plasma.

and

$$\partial u/\partial t + u(\partial u/\partial r) + (\partial p/\partial r)/\rho = 0 \qquad (2.3)$$

Also the shock front is subject to the conservation equations (4, p. 129) which, with rearrangement, become

$$u_s = [(p_1-p_o)/(1/\rho_o-1/\rho_1)]^{1/2}/\rho_o \qquad (2.4)$$

and

$$u_1 = u_s(1-\rho_o/\rho_1) \qquad (2.5)$$

where u_s is the shock velocity. The surface of the expanding cylinder is subject to the boundary conditions of continuity of pressure and zero relative mass velocity.

It is assumed that all variables depend only upon the ratio t/r designated by x, and not upon t or r separately. Then the following functional representations are made:

$$u = U(x)/x \qquad (2.6)$$

$$c = C(x)/x \tag{2.7}$$

$$p + B = P(x)/x^2 \tag{2.8}$$

$$\rho = \Omega(x) \tag{2.9}$$

The functions are related through the equation for sound velocity by

$$C^2 = \gamma P/\Omega \tag{2.10}$$

A set of differential equations can be derived in the same way as those for spherical coordinates given by Taylor. For cylindrical coordinates they are

$$D \times \partial U/\partial x = U[(1-U)^2-2C^2] \tag{2.11}$$

$$D \times \partial C/\partial x = C[(1-U)^2-C^2-(\gamma-1)U(1-U)/2] \tag{2.12}$$

$$D \times \partial \Omega/\partial x = \Omega U(1-U) \tag{2.13}$$

where

$$D = (1-U)^2 - C^2 \tag{2.14}$$

Dividing (2.12) by (2.11) gives a first-order ordinary differential equation:

$$\frac{dC}{dU} = \left(\frac{C}{U}\right) - \frac{(1-U)^2-C^2-(\gamma-1)U(1-U)}{(1-U)^2-2C^2} \tag{2.15}$$

If the differential equation is solved for C as a function of U, all the variables can then be found as functions of x by quadratures.

The starting point for calculating a particular data point is a pair of values for ambient pressure p_0 and shock front pressure p_1. The differential equation is integrated numerically, subject to the boundary conditions, from the shock front to the surface of the expanding cylinder. Then quadratures are performed, and the values of cylinder expansion rate, cylinder pressure, and other unknowns are obtained.

The calculations have been performed by a computer for a wide range of starting conditions; the results are shown in Fig. 4. Each curve shows the variation in the cylinder pressure with expansion rate for a particular value of ambient pressure. However, the calculation was not completely successful. The dashed line for 100 kilobars illustrates what would be expected from physical intuition, that the pressure would approach the ambient value as the growth rate approaches zero. Yet the computer solution shows a deviation from that trend for small values of growth rate. The cause of the deviation is thought to be the mathematical assumption that t/r is the only independent variable.

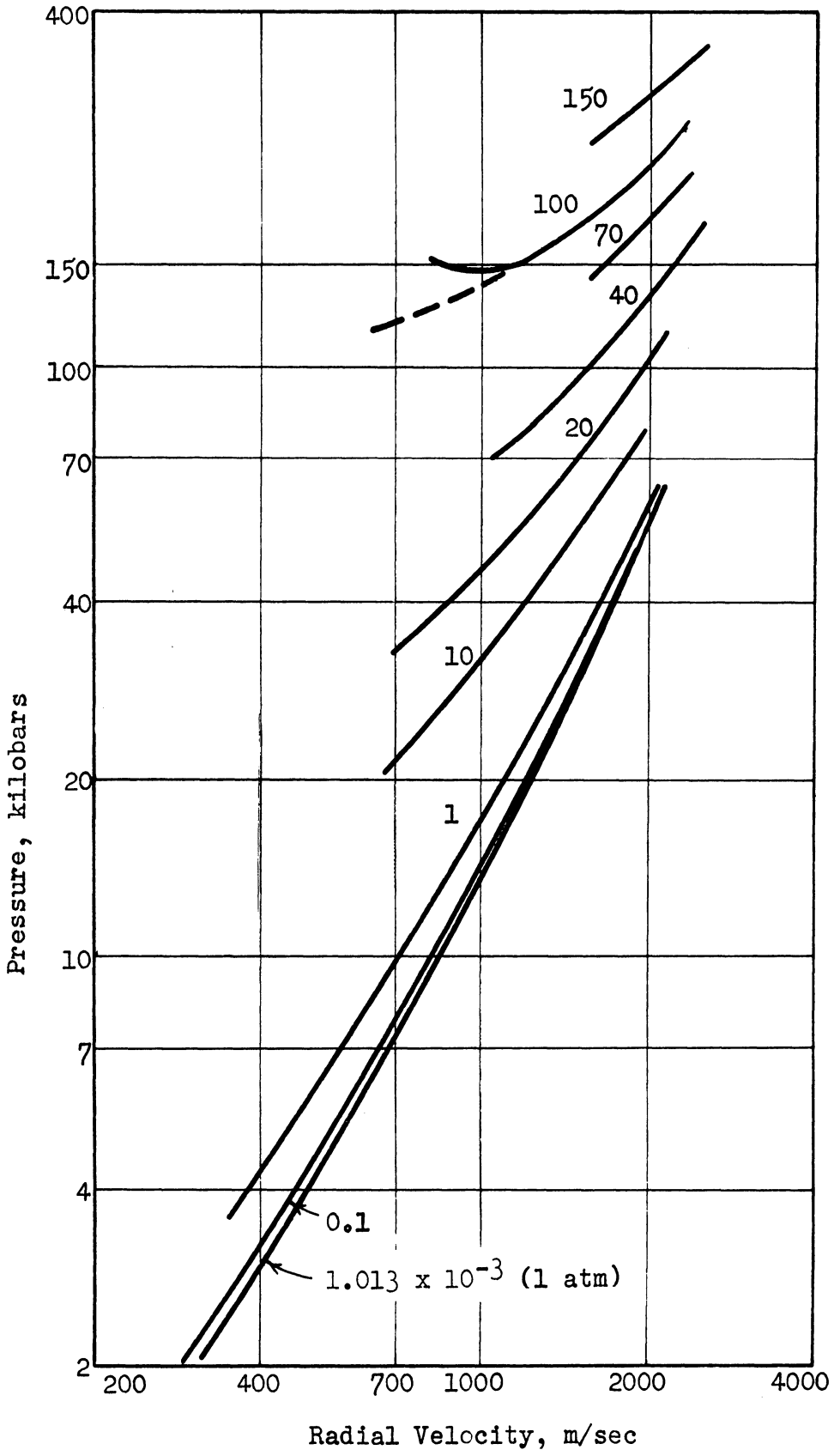

Fig. 4. Results of computer calculation of pressure on expanding cylinder in water for various values of ambient pressure.

C. L. Dolph (5) has suggested a variational method which might be used instead of the method described here. The principal problem in applying his method is in properly treating the boundary conditions.

Certain modifications are necessary before a solution such as that shown in Fig. 4 is applied to a computation of pressure. Because of the induction of water into the plasma column, the displacement rate of water is less than the apparent growth rate of the column. If n is the density of atoms in the plasma, and n_o the ambient density in the water, then the measured growth rate of the plasma column should be corrected by the factor

$$1 - (n/n_o)^{1/2} \tag{2.16}$$

before the pressure is computed.

Also if the pressure is not uniform throughout the plasma, a modification would be needed to determine the average pressure from the pressure on the boundary. Such a correction would have a very minor effect on the results to be presented.

For experiments with explosive, the effect of column expansion rate was neglected altogether, and the mechanical pressure was assumed to be the ambient pressure of 100 kilobars. When the growth rate correction (2.16) was applied, the effective growth rate was so small that the effect of expansion was negligible.

One other correction arises in the computation of pressure when explosive is used. A pressure gradient exists in the water which is compressed by the explosive, and it was previously estimated to be on the order of 6 kilobars/mm (1, p. 18). If the plasma is 2 mm from the shock front, its pressure is 12 kilobars less than 100, or 88 kilobars. This gradient has been neglected in computing the pressure. However since the pressure correction would be the same for all cases, the data trends are not changed by neglecting it.

Pinch Pressure

The pinch pressure is not uniform throughout the plasma; it varies from zero at the boundary to a peak on the cylindrical axis. The pressure is found as a function of radius by integrating the force on a radial increment from the boundary of radius R to an unspecified radius r, that is

$$p(r) = -\int_R^r J(r')B(r')dr' \tag{2.17}$$

where J is current density and B is magnetic flux density. If J is constant, the total current I is $J\pi R^2$ and p(r) becomes (mks units)

$$p(r) = (\mu I^2/4\pi^2R^4)(R^2-r^2) \tag{2.18}$$

When p(r) is averaged over the volume of the plasma, the result is

$$p_{av} = \mu I^2/8\pi^2R^2 \tag{2.19}$$

This is the result that is added to the mechanical pressure to obtain the average total pressure.

The resistivity of the plasma has been found to decrease with increasing pressure, so that the resistivity of the plasma is least on the axis of the discharge. Thus the current concentrates in the center instead of being uniformly distributed. Suppose therefore that the current distribution is parabolic instead of constant. Let J be given by

$$J(r) = J_o(1-r^2/R^2) \tag{2.20}$$

and the total current by

$$I = J_o\pi R^2/2 \tag{2.21}$$

Magnetic flux density B is

$$B = \mu J_o[r'/2-r'^3/4R^2] \tag{2.22}$$

Then the pinch pressure is

$$p(r) = -\int_R^r \mu J_o^2\left(\frac{r'}{2} - \frac{3r'^3}{4R^2} + \frac{r'^5}{4R^4}\right)dr' \tag{2.23}$$

or

$$p(r) = \frac{\mu I^2}{4\pi^2R^4}\left[\frac{5}{3}R^2 - 4r^2 + \frac{3r^4}{R^2} - \frac{2r^6}{3R^4}\right] \tag{2.24}$$

The peak pressure at the axis is 5/3 of the peak pressure for a uniform current distribution. When the average pressure is evaluated, however, the same result is obtained as for the case with uniform distribution, that is

$$p_{av} = \mu I^2/8\pi^2R^2 \tag{2.25}$$

Thus even though peak pressure may be underestimated, the average pressure is given quite accurately by the assumption of uniform current distribution.

III. EXPERIMENTS WITHOUT EXPLOSIVE

The results to be presented here are for times late in the period of observation, when the discharge current and plasma column radius are large and accurately measurable. For completeness, the data and calculations for the entire interval of observation are tabulated in the Appendix for each of the experimental situations. The plasma properties of energy density, pressure, resistivity, and temperature are nearly constant throughout the growth of the plasma.

The various experimental conditions were produced by controlling the rate of current rise in the discharge circuit. The maximum rate of rise was that obtained from four capacitors in parallel, making a bank of 56.1 μF. Lesser rates of rise were obtained by using less capacitance and by introducing series inductance into the discharge circuit. The charging voltage was kept at 20 kV, so that the formative time of the discharge would be uniform for all the tests.

Each data point shown in the results represents an average from several consistant experiments. The numbers given in the Appendix are averages unless stated otherwise. Deviations from average values were generally less than 10%.

Special Electrode Design

The electrode system used in the experiments without explosive, shown in Fig. 5, was somewhat simpler than that shown in Fig. 1. Because of the need to construct a new electrode system for every experiment, the saving of time with this simpler system was important. Also, the system had a lower inductance, and the electrode spacing could be adjusted more precisely. The voltage probe wire, not shown in Fig. 5, was attacted at the lower right edge of the high potential electrode; from there it ran along the underside of the ground plane to the nonexpendable 1000X probe.

Effect of Dissolved Air

Without the destructiveness of the chemical explosive, the electrode system could be placed in a small test tank requiring much less water than was needed in the tank used for experiments with explosive. Thus it became practical to heat the water to drive off dissolved air, and to cool it back to

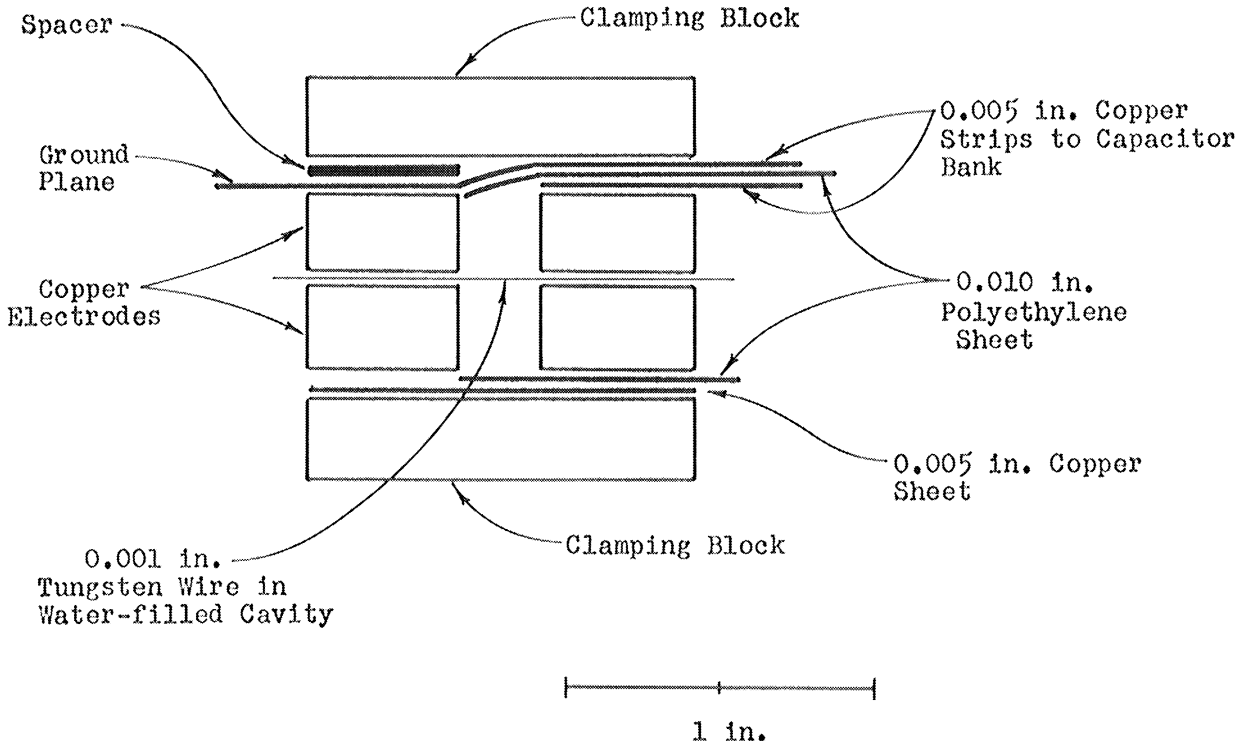

Fig. 5. Vertically exploded side view of electrode assembly for use without explosive. The rectangular electrode pieces are 3 in. long.

room temperature for the experiment. Previous tests had shown occasional irregularities which had been attributed sometimes to air bubbles and sometimes to the magnetic pinch effect. When the water was cleared of excessive dissolved air, the irregular effects were completely eliminated. The discharge columns were very regular, cylindrical structures, as shown in Fig. 6.

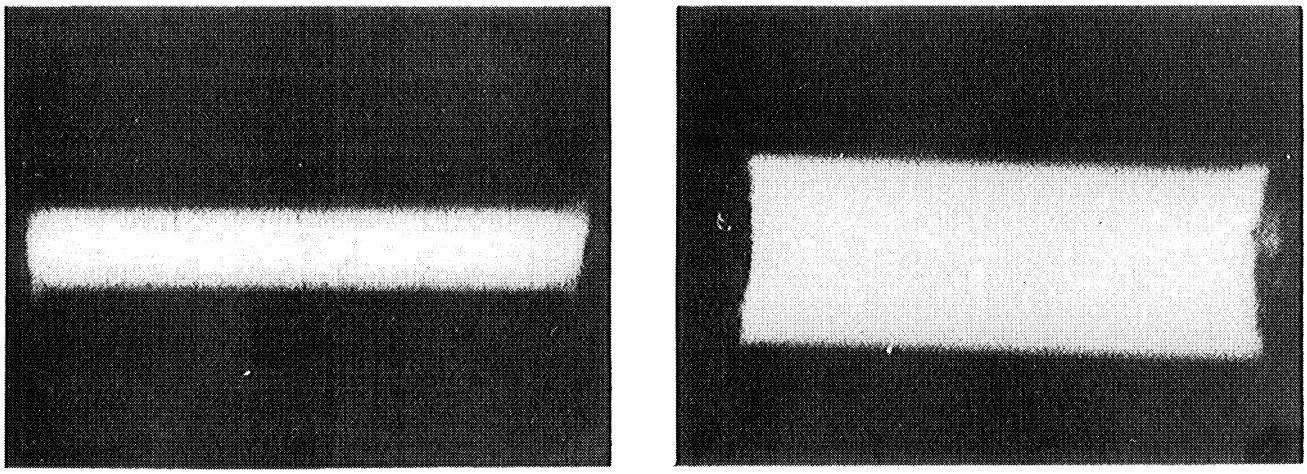

Fig. 6. Two photographs showing growth of plasma column with length of 0.240 in.

Calculations

Sweep time correction factors were determined for the oscilloscopes to eliminate effects arising from slightly different sweep speeds and to eliminate cumulative error arising in the integration of electrical power. Vertical amplifiers were calibrated when necessary.

Power was determined by correcting the voltage for inductive effects and then multiplying it by the current. The integral of the power was then divided by the volume of the plasma to obtain the energy density. Losses of energy from the plasma were neglected for these calculations, since they had been shown to be on the order of 5% for the lower rates of current rise and even smaller for higher rates (1). The losses include radiation and mechanical work of expansion against the surrounding medium.

The resistance of the plasma column can be computed from the current and the voltage, and the resistivity from the resistance and the dimensions.

Pressure was calculated by the procedures described in Section II, with the assumption of a uniform current distribution. Peak pressure on the axis is equal to the mechanical pressure plus twice the average pinch pressure. The effective growth rate for computing mechanical pressure was found by using the correction factor (2.16) and particle densities from the previous report (1, Table 13, p. 90).

Results

Results from the various experiments are compared according to the current in the discharge after 1 μsec of plasma growth. This current is very nearly equal to the rate of current rise per microsecond. Except during the formative period of the discharge, the rate of rise is nearly constant and slightly greater than the current at 1 μsec.

The growth characteristics for five different rates of rise are shown in Fig. 7. Each data point represents a single photograph of a discharge column. The time of the exposure is taken to be the end point of the 0.1 μsec interval when the shutter is open, and the diameter of the discharge column includes the outermost fringe of shading on the image. Since the column is expanding, the edge of the image is not as sharp as it would be for a shorter exposure time.

Figure 8 shows that the radius at 1 μsec approaches a limiting value of 0.8 mm as the rate of current rise increases. Since the ratio I/r is larger for larger rates of rise, the pinch pressure is more important than the pressure due to inertial confinement. Figure 9 shows pressures at 1 μsec for different rates of rise. At the higher rates the pinch dominates, and the peak

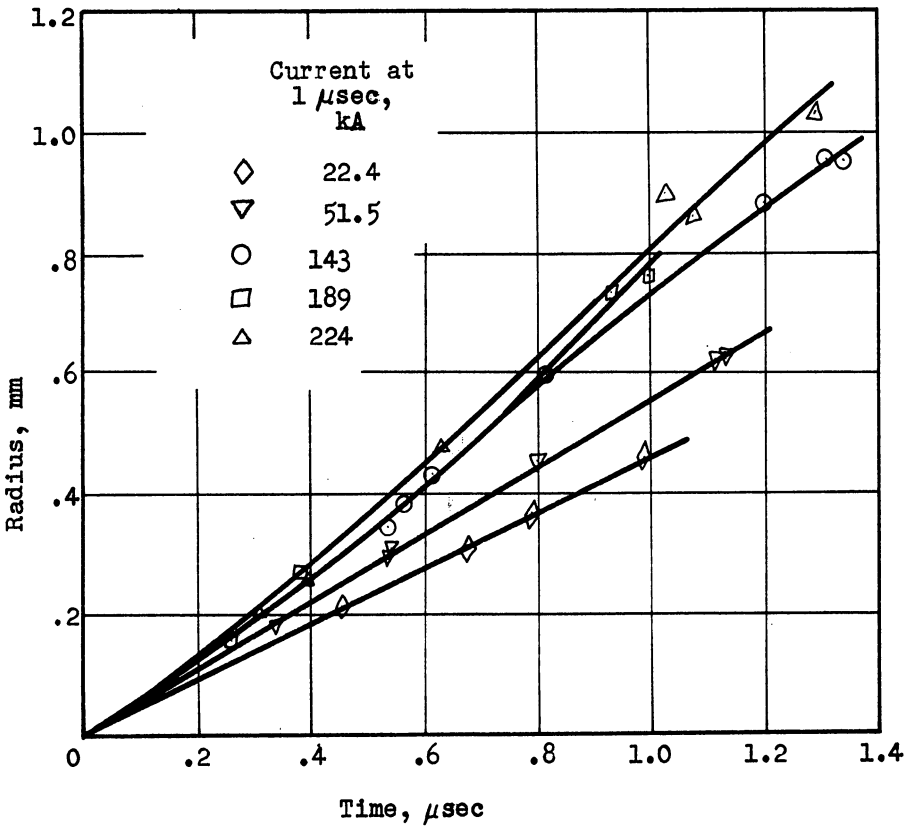

Fig. 7. Growth of discharge column when explosive is not used, with current at 1 μsec as a parameter.

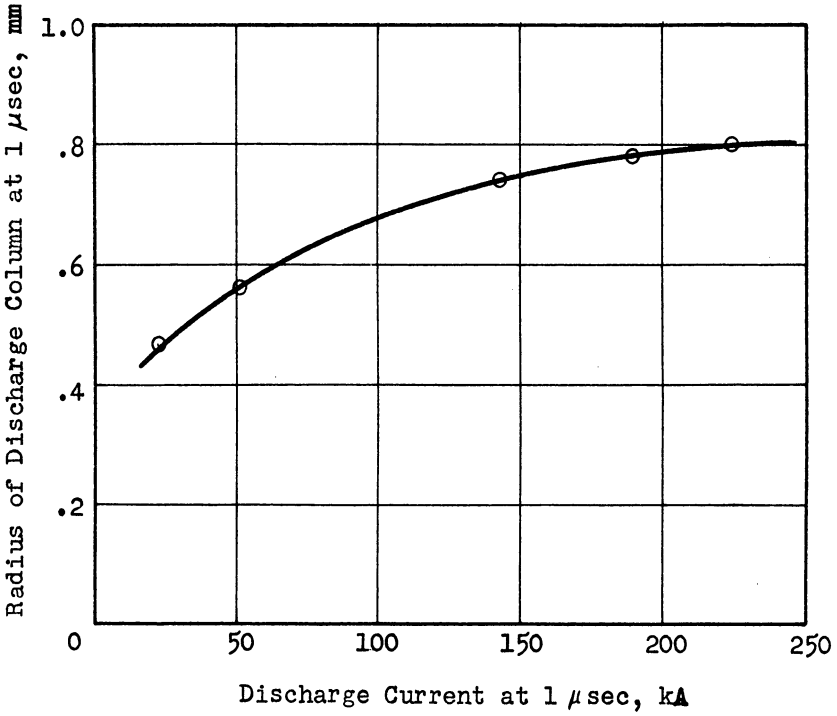

Fig. 8. Discharge column radius as a function of current at 1 μsec.

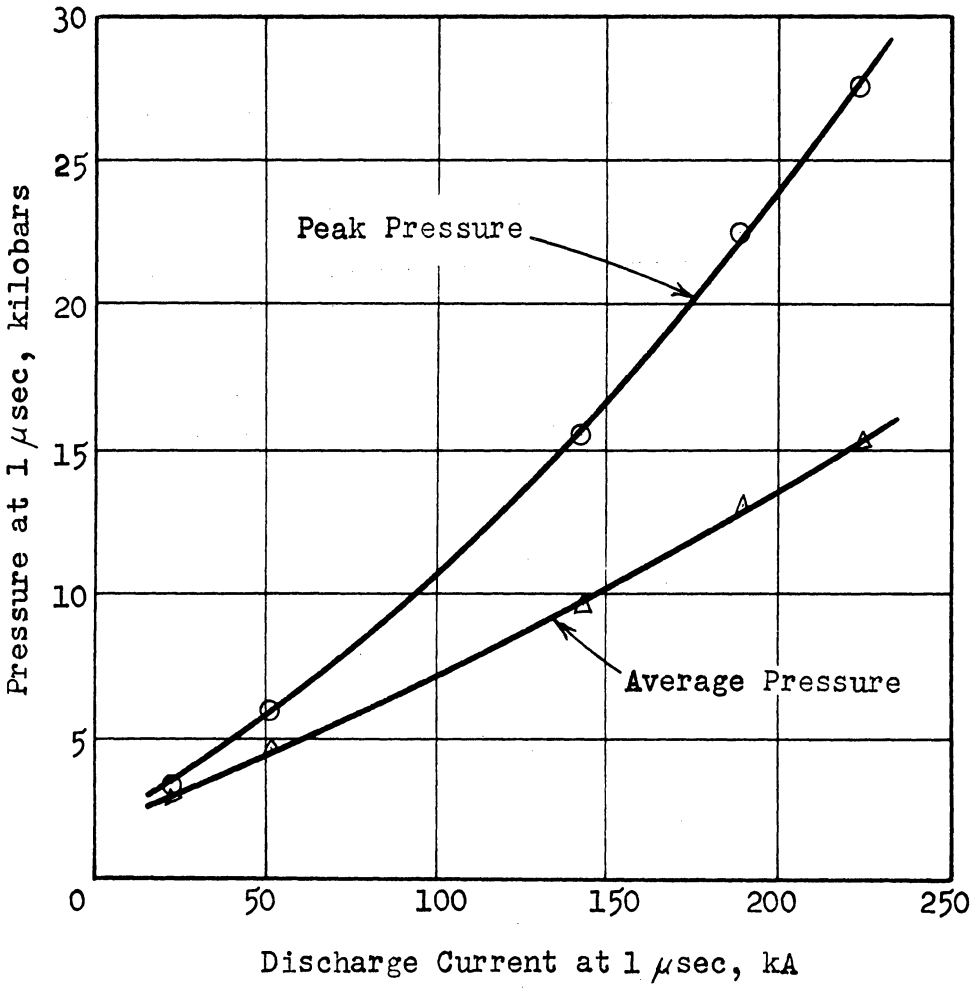

Fig. 9. Peak pressure on axis of discharge and average plasma pressure as a function of current at 1 μsec.

pressure on the axis is nearly twice the average pressure. Figure 10 shows the ratio of average pinch pressure to pressure arising from inertial restraint of the plasma by the surrounding water. The crossover point between regions where the two effects dominate is at about 10^{11} A/sec.

There were no discernible trends in temperature either with time during a given experiment, or in a comparison between experiments. In general, the temperature measurements were in the neighborhood of 35 000°K, with fairly large fluctuations. The average temperature for a given set of experimental conditions is tabulated with the rate of current rise in Table 1.

The energy density of the plasma increased with the rate of current rise, as shown in Fig. 11. When energy density is compared with pressure, the ratio of the two is nearly constant, as shown by Fig. 12. Since temperature is constant, the mass density of the plasma must also be approximately proportional to pressure.

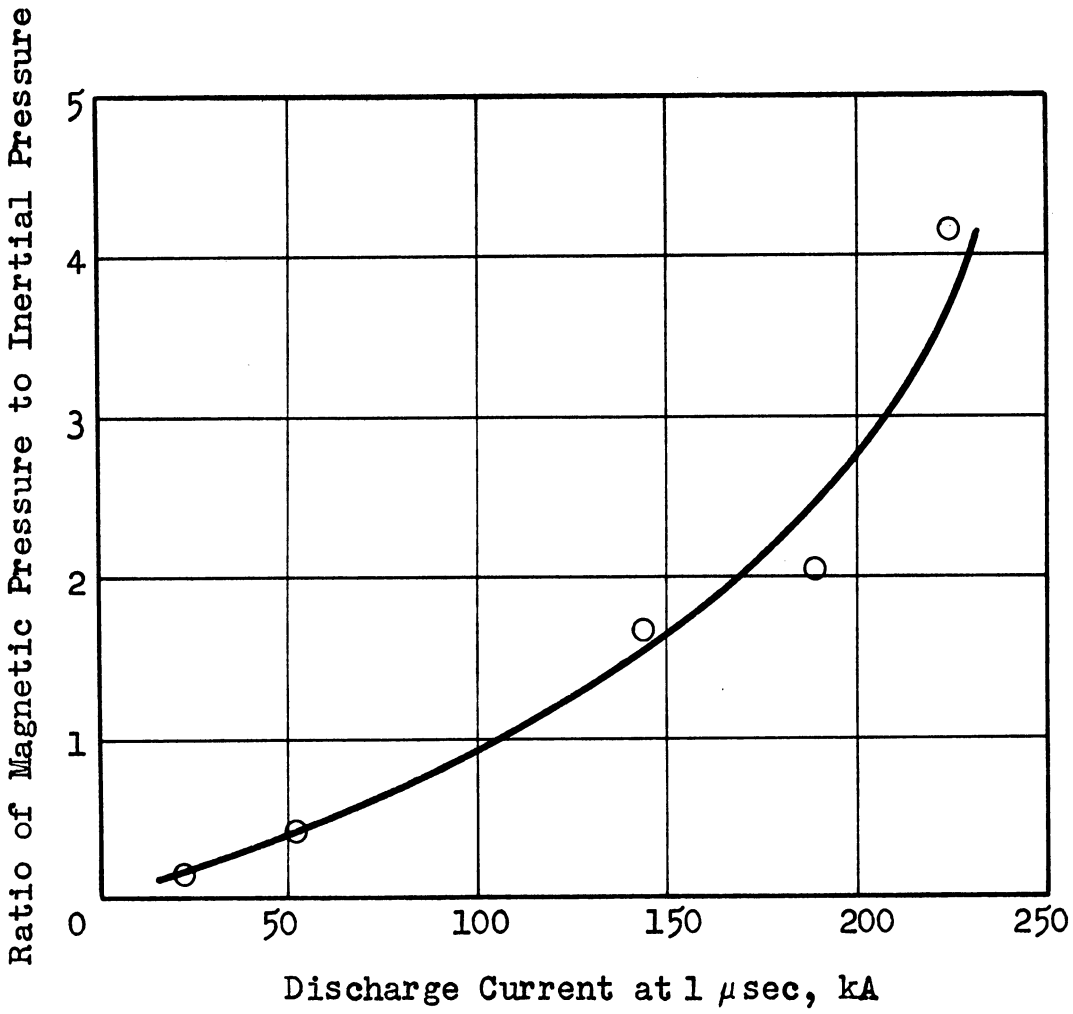

Fig. 10. Ratio at 1 μsec of magnetic pinch pressure to pressure arising from the inertial restraint of the plasma by the surrounding water.

TABLE 1

TEMPERATURE OF PLASMA COLUMN

Average Current After 1 μsec of Growth, kA	Average Temperature Determined From Photographs of Plasma, K°
22.4	34 500 ± 6000
51.5	34 500 ± 6000
143	30 500 ± 9000
189	38 500 ± 7000
224	33 000 ± 6000

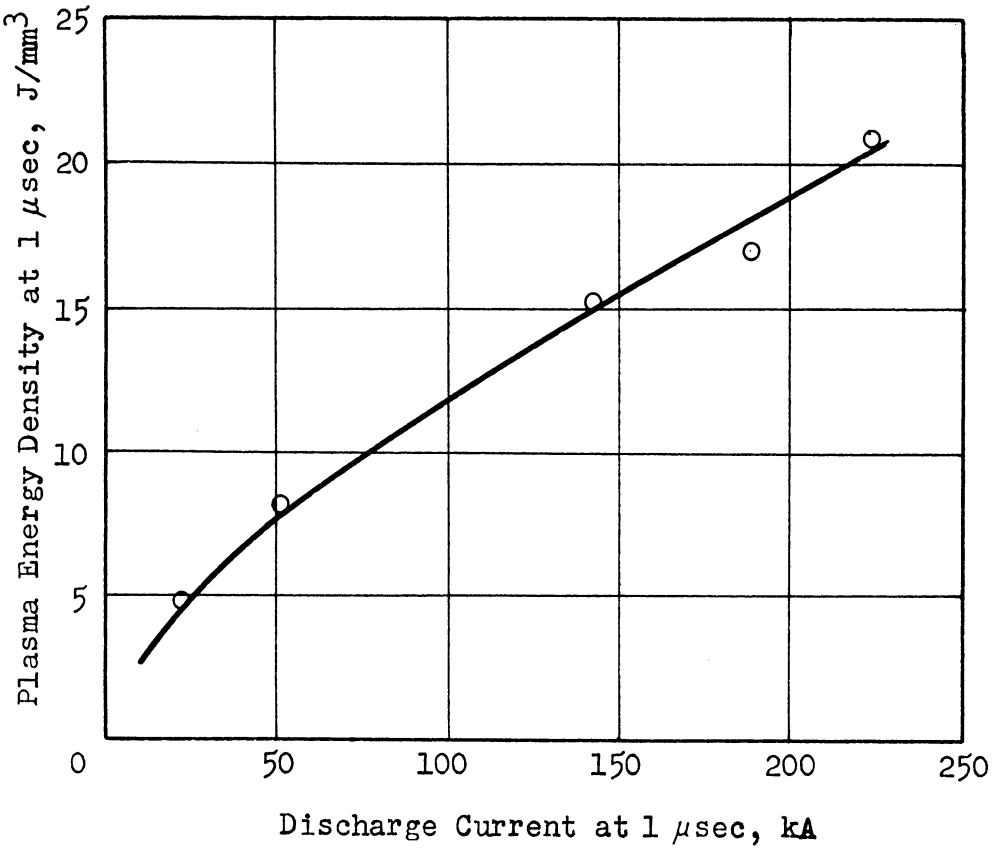

Fig. 11. Energy density at 1 μsec as a function of current.

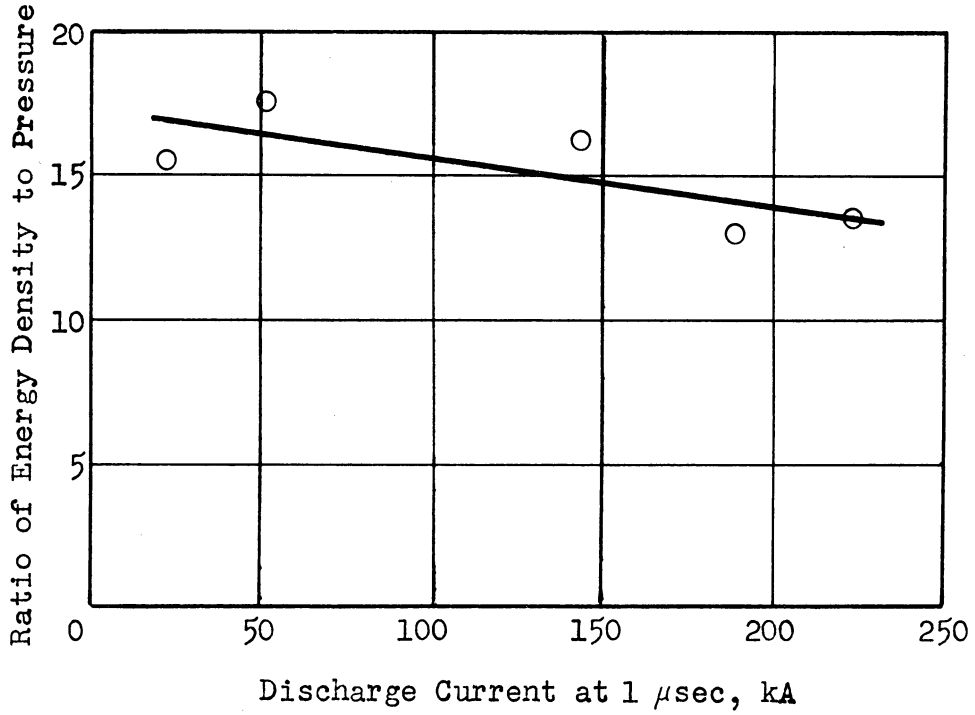

Fig. 12. Ratio at 1 μsec of energy density to pressure.

The energy density of the plasma increased with the rate of current rise, as shown in Fig. 11. When energy density is compared with pressure, the ratio of the two is nearly constant, as shown by Fig. 12. Since temperature is constant, the mass density of the plasma must also be approximately proportional to pressure.

The theoretical conclusions of the previous report are further verified by these measurements of energy density. For a pressure of 10 kilobars, the Debye shielding theory predicts an energy density of 3 J/mm^3 and an atom density of 1.6×10^{27} m^{-3}(1, p. 77). The measured value for energy density is 15 J/mm^3. The discrepancy is explained by the existence of a cohesive effect arising from the distortion of electron states, so that both particle density and energy density are much higher than predicted by the Debye theory (1, p. 88). The discrepancy applies to all of the data presented in this section.

Finally, Figs. 13 and 14 show the variation of plasma resistivity with

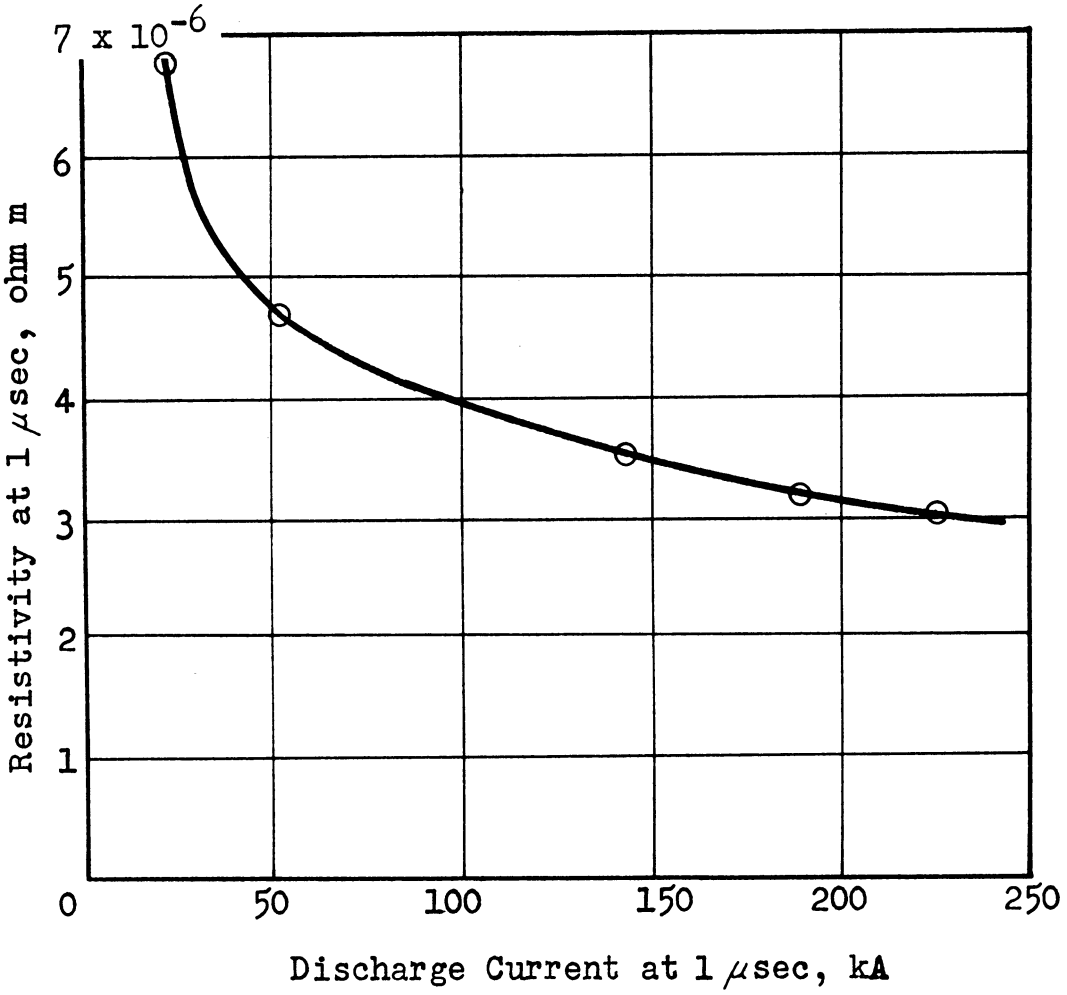

Fig. 13. Plasma resistivity as a function of current at 1 μsec.

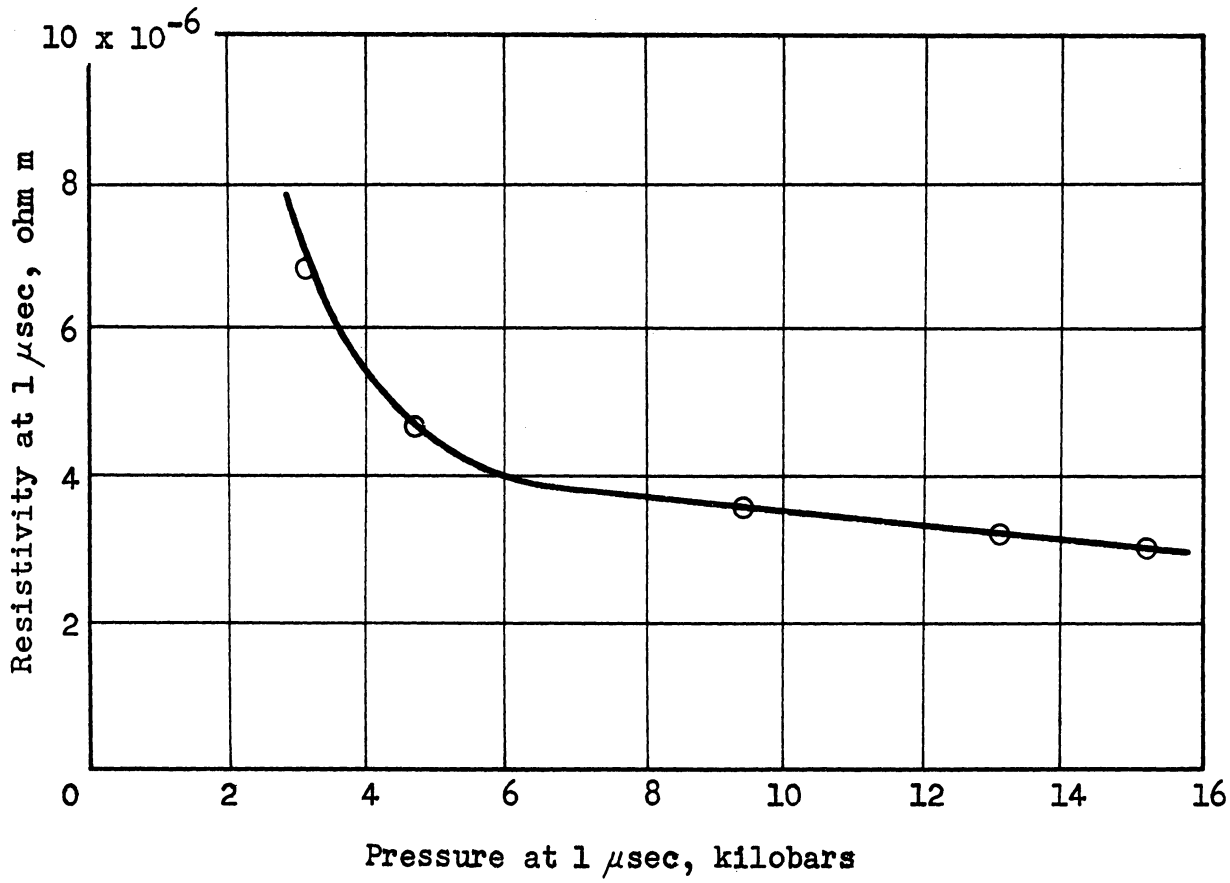

Fig. 14. Plasma resistivity as a function of pressure at 1 μsec.

rate of current rise and pressure. Resistivity was found to decrease with an increase of pressure, so that the current tends to concentrate at the axis of the discharge when a strong pinch effect produces a high peak pressure on the axis.

IV. EXPERIMENTS WITH EXPLOSIVE

The same general remarks apply to this section as to the preceding one. The procedures and calculations, tabulated in the Appendix, are the same, with minor exceptions. For these experiments the electrode system of Fig. 1 was used.

Events were so timed that the shock wave from the chemical explosive passed over the initiating wire at the time when the discharge was initiated, or slightly before. Thus the plasma column was developed in a region of fairly uniform pressure. In the earlier work (1), the shock wave compressed the column after it had formed, and flattened its cross section from a cylinder. In the present work, however, there was no flattening, because the water was compressed before the discharge began.

Calculations

In the calculation of energy density, the energy lost from the plasma by the mechanical work of expansion was taken into account. The loss was greater then for the cases without explosive because of the higher pressure. The change of volume of the plasma is caused partially be displacement of the surroundings and partially by induction of water into the plasma. For computing work, therefore, a corrected volume must be used. If n is the density of atoms in the plasma and n_o the density of atoms in water compressed to the ambient value of 100 kilobars, then a change of volume should be corrected by the factor $(1-n/n_o)$ where n_o is 1.6×10^{29} m^{-3}. With a value for n of 10^{29}, as previously estimated (1), the correction factor is 0.375. Thus for a constant pressure of 100 kilobars around the plasma column, the work is $0.375 \int p\, dV$, or simply 0.375 p V. The energy loss is still not a large fraction of the total energy.

As was explained in Section II, the pressure for these experiments is simply the ambient pressure, 100 kilobars, plus the magnetic pinch pressure. Once again a uniform current distribution is assumed for computing pinch pressure. The effects of the pressure gradient have been neglected.

Results

As in the results of the preceding section, one might choose the rate of current rise as the basis for comparing the different experiments. But com-

plications arise, because the rates are the same for the tests with two and with four capacitors, and the voltages are different. It was more convenient to choose pressure as the basis for comparison, where pressure is 100 kilobars plus the average pinch pressure.

Three tests were completed with the full bank of four capacitors, but each yielded different data. (With smaller amounts of capacitance the tests were consistent and reproducible.) Since there were no indications of malfunctions in the equipment, the differences may be related to the nature of the plasma itself. It is suspected that for a certain rate of current rise, there is a transition in the effect of the pinch pressure upon the discharge. Of the three tests, one yielded data similar to those obtained with two capacitors, and that test is not considered further. One yielded data that were a logical extension of the data from the tests with less than full capacitance, and the third was inconsistent with any of the other data. The inconsistent data point is shown by a unique symbol on the graphs of results to follow.

The growth of the discharge column radius with time is shown in Fig. 15.

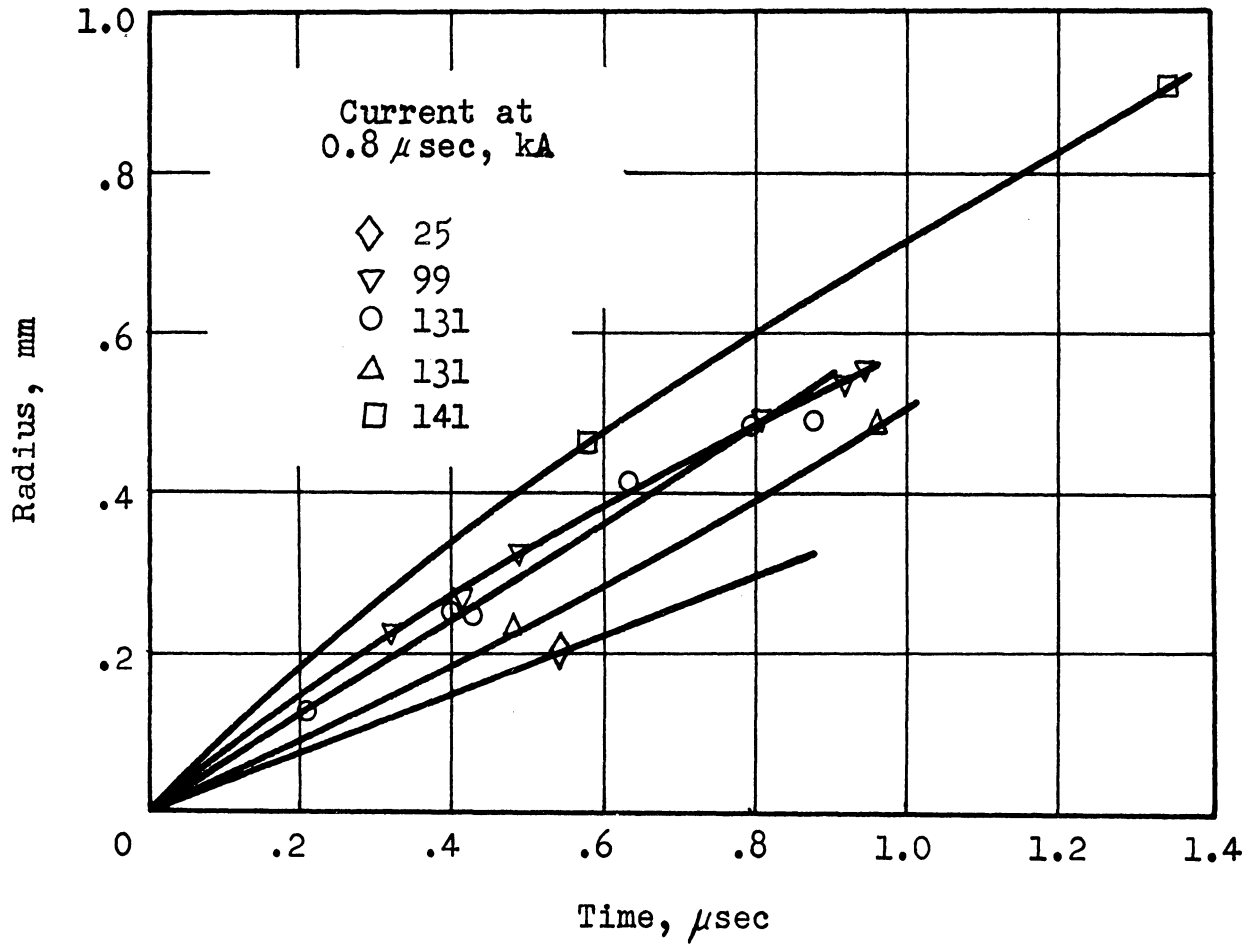

Fig. 15. Growth of discharge column when explosive is used, with current at 0.8 μsec as a parameter.

The trace identified with the symbol □ grows more rapidly than any of the others, and it is the one which is inconsistent, as will be seen. Radius is compared with pressure in Fig. 16 for the various tests in which the data

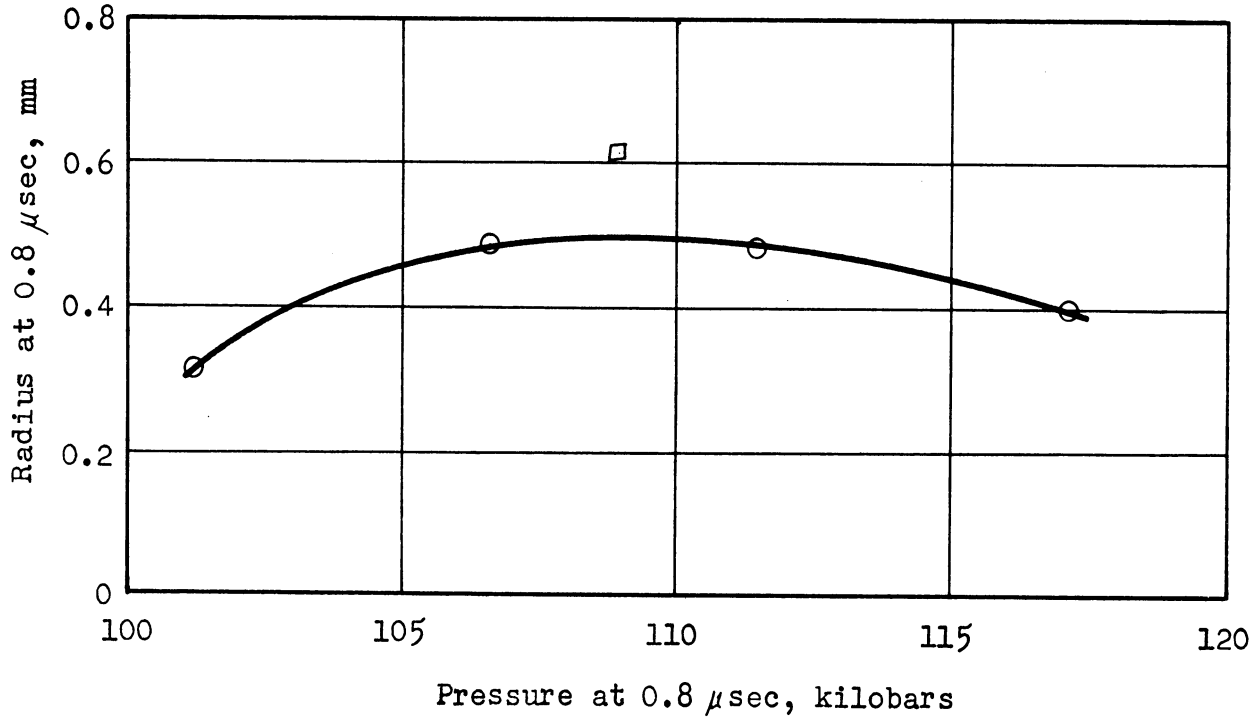

Fig. 16. Relation between plasma column radius and pressure at 0.8 μsec.

points were evaluated for a point in time 0.8 μsec after the initiation of the discharges. Figure 17 shows current at 0.8 μsec as a function of pressure.

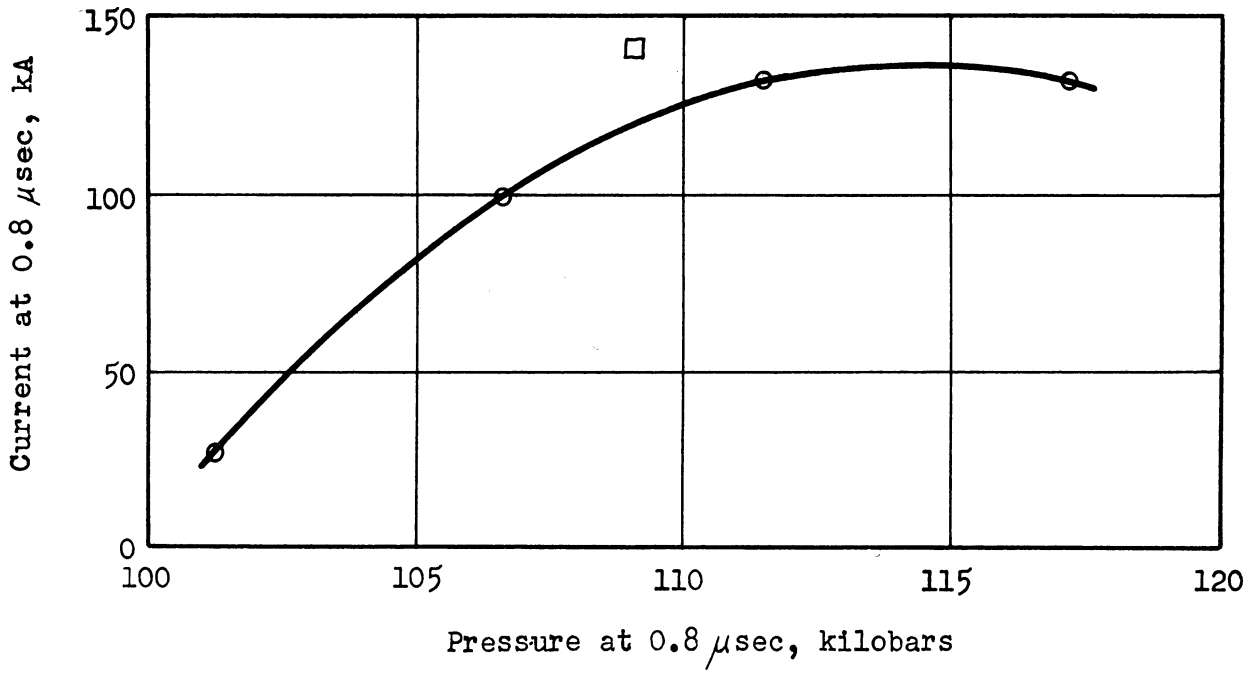

Fig. 17. Relation between discharge current and pressure at 0.8 μsec.

Energy density and resistivity are shown as functions of pressure in Figs. 18 and 19.

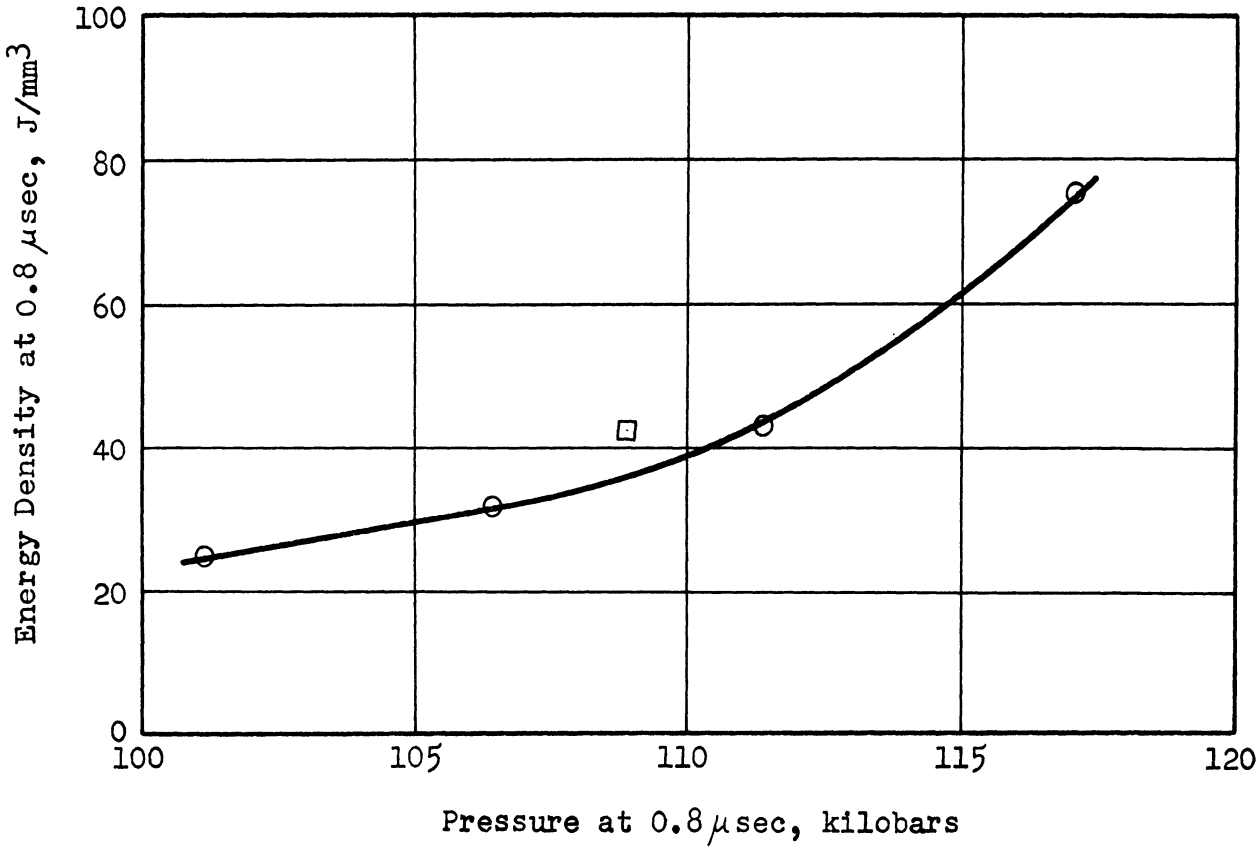

Fig. 18. Plasma energy density as a function of pressure at 0.8 μsec.

In all of the graphs in which pressure is the abcissa, the point at 117 kilobars represents the test with full capacitance, which is the logical extension of the other data. Because of the pinch effect, the rate of column growth is less than what it would be with less capacitance, and energy density reaches a very high value.

Although no firm conclusions can be based on the inconsistent data point, some explanations can be suggested. From Fig. 18, the point is found to be nearly consistent with energy density data, so as to confirm the measurements. Possibly there is a bistable condition in which a strong pinch either does or does not develop, according to the formative processes of the discharge column. On the other hand, there may be a critical rate of current rise below which a strong pinch effect develops, and above which the pinch loses its restraining power on the growth of the column because of the extremely high energy density which would develop.

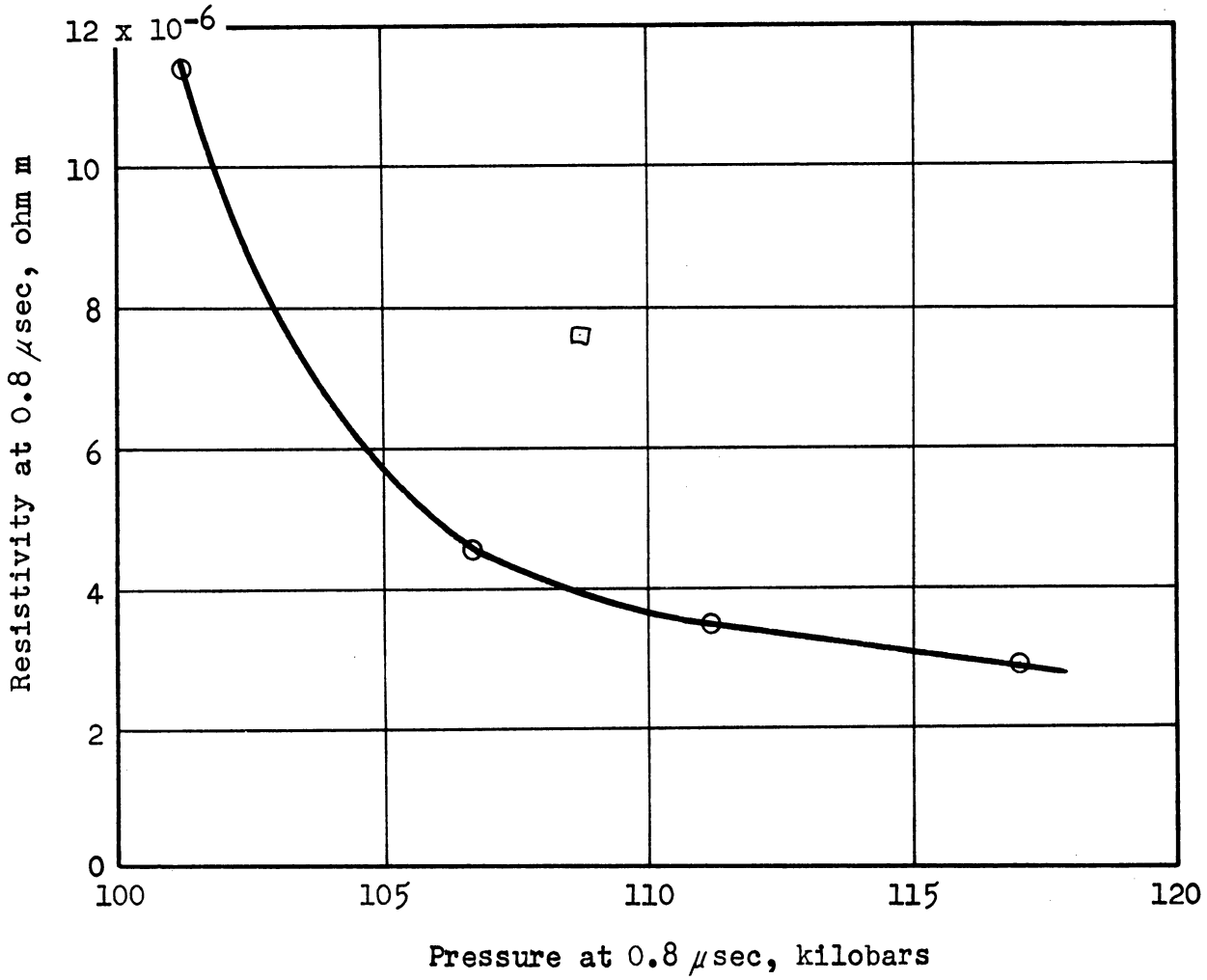

Fig. 19. Plasma resistivity as a function of pressure at 0.8 μsec.

Irregularities

Temperature is discussed in this section, separately from the other results, because of the irregular temperature patterns which develop in the discharge columns. The measured values of temperature ranged from 8000°K to 12 000°K; the temperature differences were observed in comparing different discharges and, in some cases, in comparing different regions in a single discharge. There was no apparent trend relating temperature to the other variables such as energy density. Some of the differences from one experiment to another can be attributed to variations in exposure or development of the film, but not the differences within a single photograph.

Generally the columns had fairly uniform shapes, so that dimensions could be determined for the purposes of calculating results like those in the preceding graphs. In the experiments reported earlier (1, p. 98), the shapes were

much less regular, probably because the system of electrodes used allowed the shock wave to diverge from the end of the explosive instead of keeping it confined, and thus allowed the pressure from the explosive to fall rapidly. The electrode system shown in Fig. 1 confined the shock wave, and the shape of the column was more regular.

One fairly common type of irregularity is shown in Fig. 20, where a hot

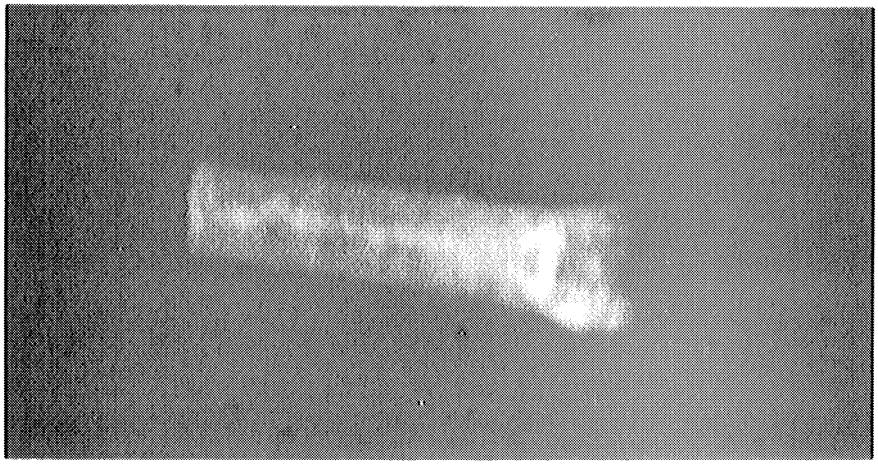

Fig. 20. Photograph of plasma column, formed with the use of explosive, showing an irregular temperature pattern.

streak has developed. Figure 21 shows a densitometer tracing of the plasma

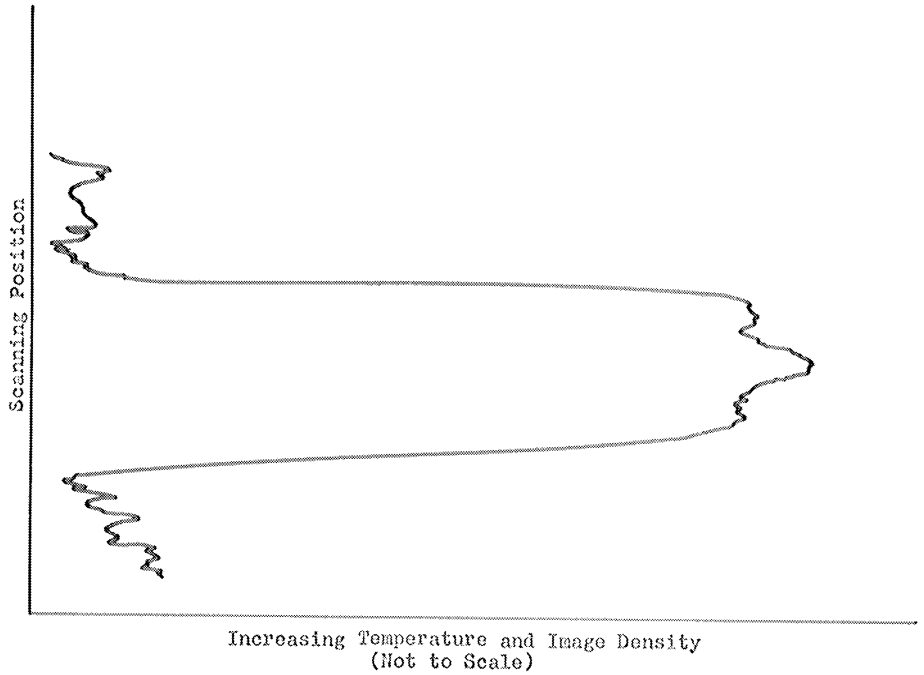

Fig. 21. Microdensitometer scan of the negative from which Fig. 20 was printed. The direction of scanning was normal to the axis of the discharge.

column image with the direction of traverse normal to the axis of the column. The lower temperature was 7700°K; the higher was 8500°K. Since the plasma is considered an opaque blackbody radiator, the hot streak suggests the existence of a very hot core with such strong radiation that it becomes visible through the absorbing outer layer. On occasion the hot streak did not run the length of the column, but faded out on one end, as shown in Fig. 22.

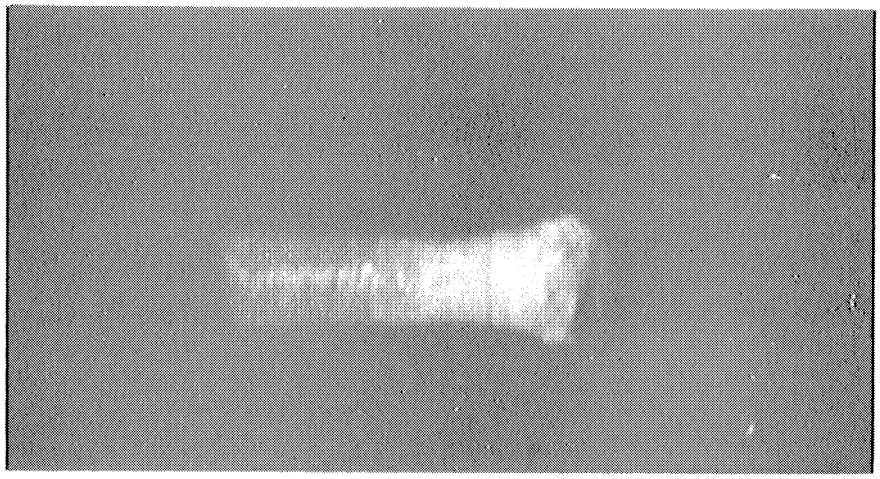

Fig. 22. Another example of irregular temperature formation.

Another common irregularity is a cool streak in the discharge column, as shown in Fig. 23. For this case, the temperature profile ranged from 8500°K to 12 000°K.

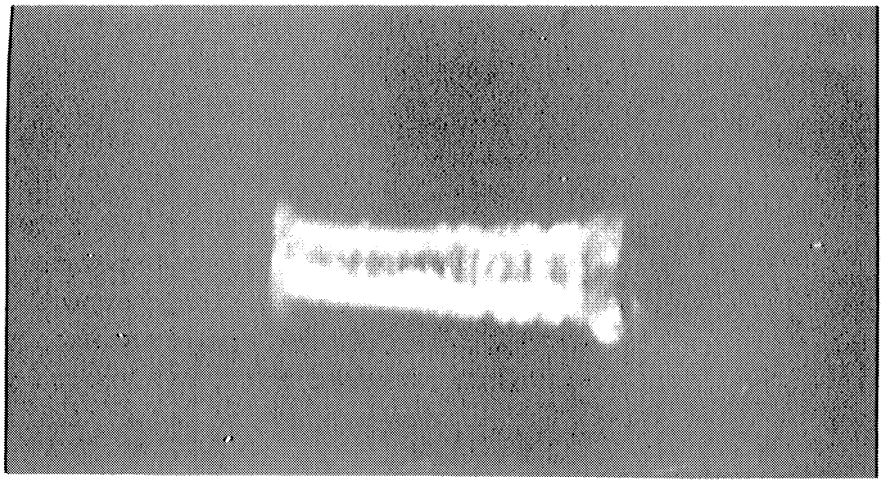

Fig. 23. A different type of irregular temperature pattern.

CONCLUSIONS

For an experiment with no explosive, the rate of current rise in the discharge column determines the pressure, which varied from 3 to 15 kilobars in these studies. For low rates, the pressure is produced by the inertial restraint of the water which surrounds the column; for higher rates, the growth rate is not correspondingly higher, and the magnetic pinch pressure dominates. The crossover point was at a rate of current rise of 10^{11} A/sec. Energy density increases in nearly constant ratio with pressure, with energy density being 15 J/mm^3 at 10 kilobars. A system of equations based upon the Debye shielding theory predicts energy density from temperature and pressure to be about 1/5 of the measured value. The theoretical prediction of mass density is also low. The proper analysis requires the use of quantum theory to treat the strong interactions between the closely spaced particles. For experiments without explosive, the temperature is about 35 000°K, which is independent of the rate of current rise. The resistivity of the plasma decreases with increasing pressure, and has a value of 3.5×10^{-6} ohm m at 10 kilobars. Since the magnetic pinch pressure is greater on the axis of the discharge column than at the outside, the current tends to concentrate on the axis so that the pinch effect is intensified.

For experiments with explosive, the rate of current rise affects the pressure. Trends in the data are related to the pinch pressure, which is superimposed upon the base pressure of 100 kilobars produced by the explosive. Energy density is an increasing function of pressure, but not proportionally as for the data taken without explosives. A peak of 75 J/mm^3 was attained at 117 kilobars. The resistivity again shows a decrease with increasing pressure, where it has a value of 3.5×10^{-6} ohm m at 110 kilobars. Plasma temperature is approximately 10 000°K regardless of the rate of current rise, and nonuniform temperature patterns develop in the discharge columns.

APPENDIX

The ten tables in this section present the numerical calculations for the experiments which form the basis of this report. The notations in the tables are defined as follows:

A	Cross sectional area of plasma column
d	Length of plasma column
E	Electrical energy
I	Discharge current
p_i	Pressure from inertial restraint of expanding plasma column
p_m	Magnetic pinch pressure averaged over volume
p_p	Peak pressure on axis of discharge column
r	Radius of discharge column
R	Resistance of plasma column
ρ	Resistivity of plasma
t	Time measured from initiation of discharge
u	Energy density of plasma
V	Voltage corrected for inductive effects
W	Mechanical work done by expanding plasma

TABLE 2

AVERAGE DATA FOR SET OF EXPERIMENTS WITHOUT EXPLOSIVE

(13.7 μF at 20 kV with added series inductance, discharge path of 6.1 mm)

t, μsec	I, kA	V, kV	r, mm	A, mm^2	E/d, J/mm	u, J/mm^3	p_i, kilobars	p_m, kilobars	p_p, kilobars	R/d, ohm/m	ρ, ohm m
0.0	0.0	--	0.0	0.0	0.0	--	--	--	--	--	--
.1	--	--	--	--	--	--	--	--	--	--	--
.2	2.7	4.50	0.091	0.0260	0.251	9.66	2.75	--	--	--	--
.3	4.8	3.40	.138	.0598	.478	7.99	2.75	0.193	3.14	--	--
.4	7.2	2.70	.184	.106	.788	7.34	2.75	.243	3.24	--	--
.5	9.6	2.27	.232	.169	1.13	6.68	2.75	.272	3.29	--	--
.6	12.2	1.97	.279	.245	1.52	6.18	2.75	.304	3.36	26.8	6.57×10^{-6}
.7	14.7	1.73	.325	.332	1.92	5.78	2.75	.325	3.40	19.7	6.53
.8	17.3	1.55	.372	.434	2.37	5.46	2.75	.345	3.44	15.2	6.61
.9	20.0	1.42	.420	.553	2.84	5.13	2.75	.362	3.47	11.8	6.53
1.0	22.6	1.33	0.465	0.679	3.32	4.88	2.75	0.377	3.50	10.0	6.79

TABLE 3

AVERAGE DATA FOR SET OF EXPERIMENTS WITHOUT EXPLOSIVE

(13.7 μF at 20 kV with added series inductance, discharge path of 6.1 mm)

t, μsec	I, kA	V, kV	r, mm	A, mm^2	E/d, J/mm	u, J/mm^3	p_i, kilobars	p_m, kilobars	p_p, kilobars	R/d, ohm/m	ρ, ohm m
0.0	0.0	--	0.0	0.0	0.0	--	--	--	--	--	--
.1	--	--	--	--	--	--	--	--	--	--	--
.2	5.8	--	0.103	0.0333	0.521	15.6	3.35	0.537	4.42	--	--
.3	11.0	3.77	.158	.0784	1.09	13.9	3.35	.772	4.89	--	--
.4	16.5	2.94	.216	.147	1.85	12.6	3.35	.927	5.20	--	--
.5	22.4	2.46	.275	.237	2.70	11.4	3.35	1.06	5.42	--	--
.6	28.2	2.13	.333	.348	3.60	10.3	3.35	1.14	5.63	12.0	4.18×10^{-6}
.7	33.8	1.89	.391	.480	4.59	9.57	3.35	1.19	5.73	9.15	4.39
.8	39.6	1.72	.450	.636	5.68	8.94	3.35	1.23	5.81	7.15	4.54
.9	45.3	1.58	.505	.801	6.84	8.54	3.35	1.28	5.91	5.75	4.61
1.0	51.1	1.48	.560	.985	8.07	8.18	3.35	1.32	5.97	4.75	4.68
1.1	56.5	1.43	0.613	1.18	9.40	7.96	3.35	1.35	6.05	4.15	4.90

TABLE 4

AVERAGE DATA FOR SET OF EXPERIMENTS WITHOUT EXPLOSIVE

(13.7 μF at 20 kV, discharge path of 6.1 mm)

t, μsec	I, kA	V, kV	r, mm	A, mm^2	E/d, J/mm	u, J/mm^3	p_i, kilobars	p_m, kilobars	p_p, kilobars	R/d, ohm/m	ρ, ohm m
0.0	0.0	--	0.0	0.0	0.0	--	--	--	--	--	--
.1	--	--	--	--	--	--	--	--	--	--	--
.2	13.5	--	--	--	--	--	--	--	--	--	--
.3	27.0	4.60	0.127	0.0507	2.47	48.8	5.3	7.18	19.7	--	--
.4	42.5	3.63	.215	.145	4.76	32.8	5.5	6.23	18.0	--	--
.5	60.0	3.04	.312	.306	7.55	24.7	5.8	5.89	17.6	--	--
.6	78.0	2.61	.405	.516	10.75	20.9	4.7	5.91	16.5	5.35	2.76×10^{-6}
.7	96.0	2.30	.495	.770	14.25	18.5	4.5	6.00	16.5	4.05	3.12
.8	113	2.07	.582	1.06	18.0	17.0	4.3	6.00	16.3	3.05	3.23
.9	128	1.91	.665	1.39	21.9	15.8	3.7	5.91	15.5	2.45	3.51
1.0	143	1.81	.740	1.72	26.1	15.2	3.5	5.94	15.4	2.05	3.53
1.1	157	1.74	.813	2.08	30.5	14.7	3.3	5.93	15.2	--	--
1.2	--	--	0.879	2.43	--	--	--	--	--	--	--

TABLE 5

AVERAGE DATA FOR SET OF EXPERIMENTS WITHOUT EXPLOSIVE

(27.6 μF at 20 kV, discharge path of 6.1 mm)

t, μsec	I, kA	V, kV	r, mm	A, mm^2	E/d, J/mm	u, J/mm^3	p_i, kilobars	p_m, kilobars	p_p, kilobars	R/d, ohm/m	ρ, ohm m
0.0	0.0	--	0.0	0.0	0.0	--	--	--	--	--	--
.1	--	--	--	--	--	--	--	--	--	--	--
.2	15.0	--	0.113	0.0402	--	--	--	--	--	--	--
.3	33.0	--	.181	.103	2.41	23.4	--	--	--	--	--
.4	55.5	3.40	.253	.201	4.79	23.8	2.8	7.66	18.1	--	--
.5	77.0	2.81	.330	.342	8.02	23.4	3.0	8.67	20.3	--	--
.6	99.5	2.52	.411	.529	11.9	22.5	3.5	9.32	22.1	4.30	2.27×10^{-6}
.7	122	2.30	.498	.780	16.3	20.9	3.7	9.62	22.9	3.23	2.52
.8	145	2.14	.588	1.091	21.4	19.7	4.1	9.72	23.5	2.50	2.71
.9	167	2.02	.681	1.461	26.9	18.5	4.3	9.60	23.5	2.03	2.95
1.0	184	1.93	0.780	1.91	32.7	17.1	4.4	8.88	22.2	1.67	3.19
1.1	208	1.86	--	--	39.0	--	--	--	--	--	--

TABLE 6

AVERAGE DATA FOR SET OF EXPERIMENTS WITHOUT EXPLOSIVE

(56.1 μF at 20 kV, discharge path of 6.1 mm)

t, μsec	I, kA	V, kV	r, mm	A, mm^2	E/d, J/mm	u, J/mm^3	p_i, kilobars	p_m, kilobars	p_p, kilobars	R/d, ohm/m	ρ, ohm m
0.0	0.0	--	0.0	0.0	0.0	--	--	--	--	--	--
.1	--	--	--	--	--	--	--	--	--	--	--
.2	15.5	--	0.115	0.0416	--	--	--	--	--	--	--
.3	36.0	--	.184	.106	4.03	38.1	2.95	6.10	15.2	--	--
.4	61.0	3.63	.262	.215	7.25	33.7	2.95	8.60	20.2	--	--
.5	87.5	3.08	.350	.385	11.26	29.3	2.95	9.95	22.9	--	--
.6	114	2.72	.440	.608	16.05	26.4	2.95	10.7	24.4	3.90	2.37×10^{-6}
.7	142	2.47	.532	.888	21.5	24.2	2.95	11.4	25.8	2.83	2.51
.8	169	2.28	.623	1.22	27.7	22.7	2.95	11.7	26.4	2.25	2.74
.9	196	2.13	.712	1.59	34.4	21.6	2.95	12.1	27.2	1.83	2.91
1.0	223	2.00	.800	2.01	41.6	20.7	2.95	12.3	27.6	1.50	3.02
1.1	247	1.88	.882	2.44	49.2	20.1	2.95	12.5	28.0	1.23	3.01
1.2	271	1.80	.962	2.91	57.2	19.6	2.95	12.6	28.2	--	--

TABLE 7

DATA FOR EXPERIMENT WITH EXPLOSIVE

(13.7 μF at 20 kV with added series inductance, discharge path of 4.98 mm)

t, μsec	I, kA	V, kV	r, mm	A, mm^2	E/d, J/mm	W/d, J/mm	u, J/mm^3	p_m, kilobars	p_p, kilobars	R/d, ohm/m	ρ, ohm m
0.0	0.0	--	0.0	0.0	0.0	0.0	--	--	100	--	--
.1	--	--	--	--	--	--	--	--	--	--	--
.2	--	--	--	--	--	--	--	--	--	--	--
.3	--	--	--	--	--	--	--	--	--	--	--
.4	6.9	--	--	--	--	--	--	--	--	--	--
.5	10.2	6.48	0.1905	0.114	2.67	0.428	19.6	0.457	100.9	--	--
.6	14.8	5.78	.228	.163	4.22	.612	22.1	.672	101.3	73.0	11.9×10^{-6}
.7	20.0	5.18	.266	.222	6.18	.832	24.1	.900	101.8	50.5	11.2
.8	25.0	4.73	.305	.293	8.43	1.10	25.0	1.16	102.3	37.5	11.4
0.9	30.0	4.34	0.343	0.369	10.9	1.38	25.9	1.05	102.1	28.5	10.5

TABLE 8

AVERAGE DATA FOR SET OF EXPERIMENTS WITH EXPLOSIVE

(13.7 uF at 20 kV, average discharge path of 4.53 mm)

t, μsec	I, kA	V, kV	r, mm	A, mm^2	E/d, J/mm	W/d, J/mm	u, J/mm^3	p_m, kilobars	p_p, kilobars	R/d, ohm/m	ρ, ohm m
0.0	0.0	--	0.0	0.0	0.0	0.0	--	--	100	--	--
.1	--	--	--	--	--	--	--	--	--	--	--
.2	12.3	--	0.133	0.0556	1.18	0.21	17.5	--	--	--	--
.3	26.5	5.18	.201	.127	3.56	.48	24.2	2.77	105.5	--	--
.4	41.0	4.23	.269	.229	6.82	.86	26.0	3.70	107.4	--	--
.5	55.5	3.62	.329	.341	10.8	1.28	27.9	4.52	109.0	--	--
.6	70.0	3.20	.386	.468	15.0	1.75	28.2	5.22	110.4	9.90	4.63×10^{-6}
.7	84.5	2.92	.438	.603	20.7	2.26	30.5	5.92	111.8	7.65	4.61
.8	98.5	2.72	.485	.738	26.5	2.77	32.1	6.57	113.1	6.10	4.51
0.9	113.5	2.58	0.530	0.883	33.0	3.31	33.6	7.29	114.6	5.00	4.32

TABLE 9

AVERAGE DATA FOR SET OF EXPERIMENTS WITH EXPLOSIVE

(27.6 μF at 20 kV, average discharge path of 4.35 mm)

t, μsec	I, kA	V, kV	r, mm	A, mm^2	E/d, J/mm	W/d, J/mm	u, J/mm^3	p_m, kilobars	p_p, kilobars	R/d, ohm/m	ρ, ohm m
0.0	0.0	--	0.0	0.0	0.0	0.0	--	--	100	--	--
.1	--	--	--	--	--	--	--	--	--	--	--
.2	17.0	6.35	0.122	0.0468	1.65	0.176	31.4	--	--	--	--
.3	33.0	5.00	.183	.105	4.61	.393	40.2	--	--	--	--
.4	51.5	4.17	.244	.187	8.85	.700	43.6	--	--	--	--
.5	71.5	3.58	.305	.292	14.3	1.10	45.2	8.75	117.5	11.3	3.30×10^{-6}
.6	91.0	3.15	.366	.421	20.6	1.58	45.2	9.85	119.7	8.05	3.39
.7	111	2.84	.427	.572	27.7	2.14	44.8	10.8	121.6	6.05	3.46
.8	131	2.62	.488	.749	35.6	2.81	43.8	11.5	123.0	4.65	3.48
.9	151	2.48	.549	.947	--	3.55	--	12.0	124.0	3.65	3.46
1.0	--	--	0.610	1.17	--	4.38	--	--	--	--	--

TABLE 10

DATA FOR EXPERIMENT WITH EXPLOSIVE

(56.1 μF at 20 kV, discharge path of 4.97 mm)

t, μsec	I, kA	V, kV	r, mm	A, mm^2	E/d, J/mm	W/d, J/mm	u, J/mm^3	p_m, kilobars	p_p, kilobars	R/d, ohm/m	ρ, ohm m
0.0	0.0	--	0.0	0.0	0.0	0.0	--	--	100	--	--
.1	--	--	--	--	--	--	--	--	--	--	--
.2	13	--	0.09	0.0255	--	0.0957	--	--	--	--	--
.3	25	--	.135	.0572	5.20	.215	87.2	5.44	110.9	--	--
.4	40	5.68	.185	.107	9.45	.402	84.5	7.46	114.9	--	--
.5	60	5.08	.237	.176	15.0	.660	81.3	10.2	120.4	--	--
.6	84	4.54	.290	.264	22.1	.990	80.0	13.3	126.6	10.6	2.80×10^{-6}
.7	107	4.08	.345	.374	30.3	1.40	77.3	15.3	130.6	7.65	2.86
.8	131	3.70	.400	.503	39.7	1.89	75.2	17.1	134.2	5.75	2.89
.9	155	3.40	.457	.655	50.0	2.46	72.6	18.3	136.6	4.50	2.95
1.0	178	3.20	0.510	0.817	61.2	3.06	71.1	19.4	138.8	3.60	2.94

TABLE 11

DATA FOR EXPERIMENT WITH EXPLOSIVE

(56.1 μF at 20 kV, discharge path of 4.65 mm)

t, μsec	I, kA	V, kV	r, mm	A, mm^2	E/d, J/mm	W/d, J/mm	u, J/mm^3	p_m, kilobars	p_p, kilobars	R/d, ohm/m	ρ, ohm m
0.0	0.0	--	0.0	0.0	0.0	0.0	--	--	100	--	--
.1	--	--	--	--	--	--	--	--	--	--	--
.2	--	--	0.18	0.102	--	0.382	--	--	--	--	--
.3	28	--	.26	.212	6.28	.795	25.9	1.85	103.7	--	--
.4	46	5.86	.337	.357	11.5	1.34	28.6	2.96	105.9	--	--
.5	69	5.36	.407	.520	18.6	1.95	31.9	4.57	109.1	16.2	8.42×10^{-6}
.6	93	5.03	.463	.674	27.5	2.53	37.1	6.42	112.8	11.5	7.76
.7	117	4.75	.533	.892	38.4	3.34	39.4	7.68	115.4	8.75	7.80
.8	141	4.50	.595	1.11	51.3	4.16	42.4	8.93	117.8	6.80	7.55
.9	164	4.28	.653	1.34	66.0	5.02	45.5	10.0	120.0	5.55	7.43
1.0	188	4.09	.707	1.57	82.2	5.88	48.6	11.3	122.6	4.65	7.30
1.1	--	--	0.763	1.83	--	6.87	--	--	--	--	--

REFERENCES

1. Robinson, James W.: Measurement and Interpetation of Plasma Properties to 100 Kilobars of Pressure. NASA CR-446, 1966.

2. Martin, E. A.: Experimental Investigation of a High-Energy Density, High-Pressure Arc Plasma. J. Appl. Phys., vol. 31, 1960, p. 255-267.

3. Walsh, J. M.; Rice, M. H.: Equation of State of Water to 250 Kilobars. J. Chem. Phys., vol. 26, 1957, pp. 824-830.

4. Courant, R.; Friedrichs, K. O.: Supersonic Flow and Shock Waves. Interscience, New York, 1948.

5. Dolph, C. L.; Richardson, John M.: A Note on Variational Principles for Unsteady Compressible Flows in One Dimension. J. Inst. Maths Applics, vol. 1, 1965, pp. 113-117.